2009

Realization Of Power Factor Correction And Maximum Power Point Tracking For Low Power Wind Turbines

Gustavo Gamboa
University of Central Florida

REALIZATION OF POWER FACTOR CORRECTION AND MAXIMUM POWER POINT TRACKING FOR LOW POWER WIND TURBINES

by

Gustavo Gamboa
B.S. University of Central Florida, 2007

A thesis submitted in partial fulfillment of the requirements
for the degree of Master of Science
in the School of Electrical Engineering and Computer Science
in the College of Engineering and Computer Science
at the University of Central Florida
Orlando, Florida

Summer Term
2009

Major Professor:
Issa Batarseh

Abstract

In recent years, wind energy technology has become one of the top areas of interest for energy harvesting in the power electronics world. This interest has especially peaked recently due to the increasing demand for a reliable source of renewable energy. In a recent study, the American Wind Energy Association (AWEA) ranked the U.S as the leading competitor in wind energy harvesting followed by Germany and Spain. Although the United States is the leading competitor in this area, no one has been able successfully develop an efficient, low-cost AC/DC convertor for low power turbines to be used by the average American consumer.

There has been very little research in low power AC/DC converters for low to medium power wind energy turbines for battery charging applications. Due to the low power coefficient of wind turbines, power converters are required to transfer the maximum available power at the highest efficiency. Power factor correction (PFC) and maximum power point tracking (MPPT) algorithms have been proposed for high power wind turbines. These turbines are out of the price range of what a common household can afford. They also occupy a large amount of space, which is not practical for use in one's home. A low cost AC/DC converter with efficient power transfer is needed in order to promote the use of cheaper low power wind turbines. Only MPPT is implemented in most of these low power wind tur-

bine power converters. The concept of power factor correction with MPPT has not been completely adapted just yet.

The research conducted involved analyzing the effect of power factor correction and maximum power point tracking algorithm in AC/DC converters for wind turbine applications. Although maximum power to the load is always desired, most converters only take electrical efficiency into consideration. However, not only the electrical efficiency must be considered, but the mechanical energy as well. If the converter is designed to look like a purely resistive load and not a switched load, a wind turbine is able to supply the maximum power with lower conduction loss at the input side due to high current spikes. Two power converters, VIENNA with buck converter and a Buck-boost converter, were designed and experimentally analyzed. A unique approach of controlling the MPPT algorithm through a conductance G for PFC is proposed and applied in the VIENNA topology. On the other hand, the Buck-boost only operates MPPT.

With the same wind profile applied for both converters, an increase in power drawn from the input increased when PFC was used even when the power level was low. Both topologies present their own unique advantages. The main advantage for the VIENNA converter is that PFC allowed more power extraction from the turbine, increasing both electrical and mechanical efficiency. The buck-boost converter, on the other hand, presents a very low component count which decreases the overall cost and volume.

Therefore, a small, cost-effective converter that maximizes the power transfer from a small power wind turbine to a DC load, can motivate consumers to utilize the power available from the wind.

Hard work and dedication always pays off!

Acknowledgments

I would like to thank all the people and organization who helped make this project possible. I would like to thank my adviser Dr. Issa Batarseh for all his support through out the project. I would specially send my deepest gratitude to APECOR and all of its team members (John Elmes, Rene Kersten, Keith Mansfield and Michael Pepper) for helping make this project a success. Also, special thanks to Jonathan Baker and Christopher Hamilton for their hard work and long hours on this project. I am also very grateful to my committee members for their feedback on this work: Dr. Issa Batarseh, Michael Haralambous and Jiann Yuan.

TABLE OF CONTENTS

LIST OF FIGURES

LIST OF TABLES

CHAPTER 1: INTRODUCTION

A wind turbine can be defined as a machine that takes kinetic energy from the wind and converts it to mechanical energy. This machine transfers the motion to an electric generator shaft. Almost every low to medium power wind turbine is designed to supply a three phase AC where the frequency varies with the speed of the wind. However, these turbines operate with very low power coefficient averaging from .3 to .49. Therefore, an efficient three phase AC/DC converter with MPPT algorithm is very much needed for these types of applications when charging a DC battery supply. According to the American Wind Energy Association (AWEA), the United States has had a massive growth of wind power generation in 2008. This means that demands for more efficient converters are growing as well.

This paper will start by introducing the design of two topologies that can be realized for the power conversion of low to medium power wind turbines and use it to efficiently charge a 12V or 24V battery. This paper will also introduce a unique way for obtaining maximum power out of a low power wind turbine. It will also explain various control loops that were added to the system in order to better protect both the converter and the wind turbine. The introduction of power factor correction in low to medium power 3 phase wind turbine is discussed in this thesis. It is important to not only focus on the electrical efficiency, but the

mechanical efficiency of the source as well. The wind turbine can behave more efficiently by making an electrical converter appear like a resistive load to the source.

Unique controls for maximum power point tracking are needed for wind turbine generators. For this application, the buck-boost appears to be one of the most favorite converters. In this thesis, two converters will be analyzed and compared. It will describe the efficiency increase when power factor correction is applied along with the unique maximum power point tracking algorithm. Both converters introduced have been successfully designed operating on the left hand side (LHS) of the power curve. This allows the turbine to spin at a much lower speed when low power is required by the battery, thus potentially replacing a mechanical break of a small turbine.

All of the control loops have been experimentally tested and results are discussed. These results include data for efficiency under different component selections in order to obtain the best tradeoff in the power loss.

CHAPTER 2: TOPOLOGY RESEARCH

In small to medium power wind turbines, a traditional three phase bridge rectification is used at the output of the generator in order to obtain DC output at the terminals. Therefore, very little research has been done in regards to finding the ideal converter that can efficiently transfer the maximum amount of power out of the generator while charging a 12V or 24V battery. The topologies that are being considered in this research for a three phase AC/DC converter for low to medium power wind turbine applications are:

- Buck-boost AC/DC converter with conventional bridge rectifier.
- VIENNA rectifier with buck converter.

These topologies are operated under two different sets of control loops. The buck-boost topology only includes MPPT as well as a typical battery charging algorithm. The MPPT algorithm controls the input voltage reference of the IVR control. The VIENNA topology introduces the concept of power factor correction and the effect it has on the overall efficiency. In this topology, the MPPT controls the reference current constant for power factor correction. With these two key differences between topologies, it is up to the designer to select the appropriate tradeoff for the design.

2.1 Buck-boost converter

The buck-boost is just one of many switching converter topologies that can be realized in these types of applications. The buck-boost converter is capable of increasing or decreasing the magnitude of the voltage. However, the output voltage polarity is reversed. Converters are considered one of the simplest converters in power electronics. This converter has a very low component count thus lowering the cost. A conventional buck-boost converter is shown in Figure 2.1. In the case of wind turbines, some generators produce a three phase AC signal while others include a six diode rectifier internally. This buck-boost converter will be able to operate with both types of turbines whereas the VIENNA converter will only work for turbines that do not include the six diode rectifier. A relationship can be obtained between the duty cycle and the input and output voltage by eq. (2.7).

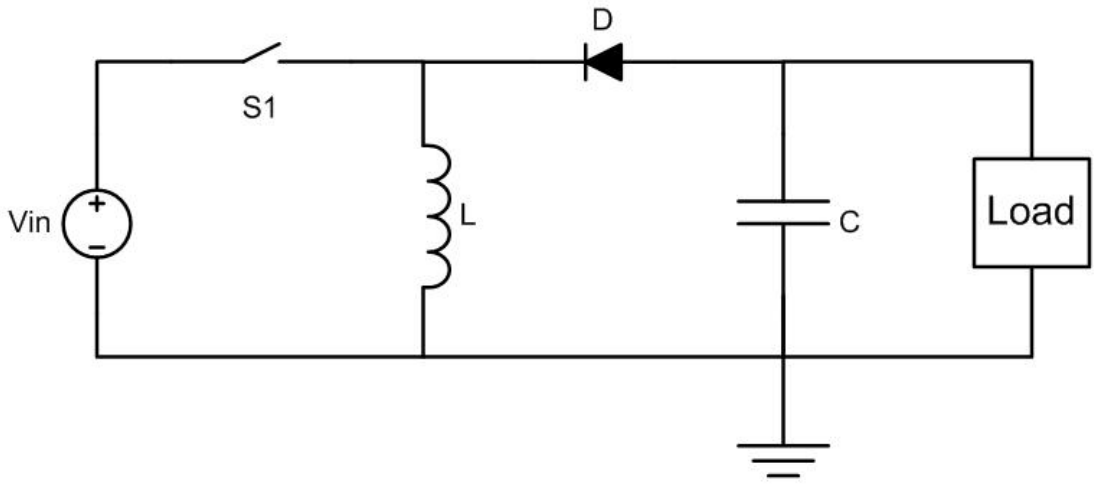

Figure 2.1: Buck-boost DC/DC converter

Because this converter's input is rectified to DC, the frequency at which it operates is much higher than the line frequency; reaching as high as a few hundred kilo-hertz. This is why these types of converter circuits are known as high frequency switching converters or regulators [Bat04]. Also, because the converter inductor current will never fall to zero during a commutation cycle, then it will be considered to be a continuous conduction mode (CCM). The other mode of operation is known as discontinuous conduction mode (or DCM) since in some cases, the load requires very little energy that is enough to be transferred in a time smaller than the whole commutation time. In terms of switching frequency, this buck-boost converter contains two modes of operation:

- $Mode1$ is defined when the converter switch is closed. This period of time is known to be from 0 to DT.
- $Mode2$ is defined when the converter switch is open. Similarly, this period of time is known to be from DT to T (also known as 0 to $(1-D)T$).

In $mode1$, shown in Figure 2.2, the input is directly connected to the inductor thus supplying current and accumulating energy. In this mode, the capacitor is disconnected from the input and it alone supplies current to the resistive load. The rate of change in the inductor current can be written as eq. (2.1). When solving for i_L throughout the time interval 0 to DT, eq. (2.2) is derived. In this equation, $I_L(0)$ is defined as the initial inductor current that corresponds to the minimum inductor current value.

$$\frac{d}{dt}I_L = \frac{V_{in}(t)}{L} \tag{2.1}$$

$$i_L = \frac{V_{in} DT}{L} + I_L(0) \tag{2.2}$$

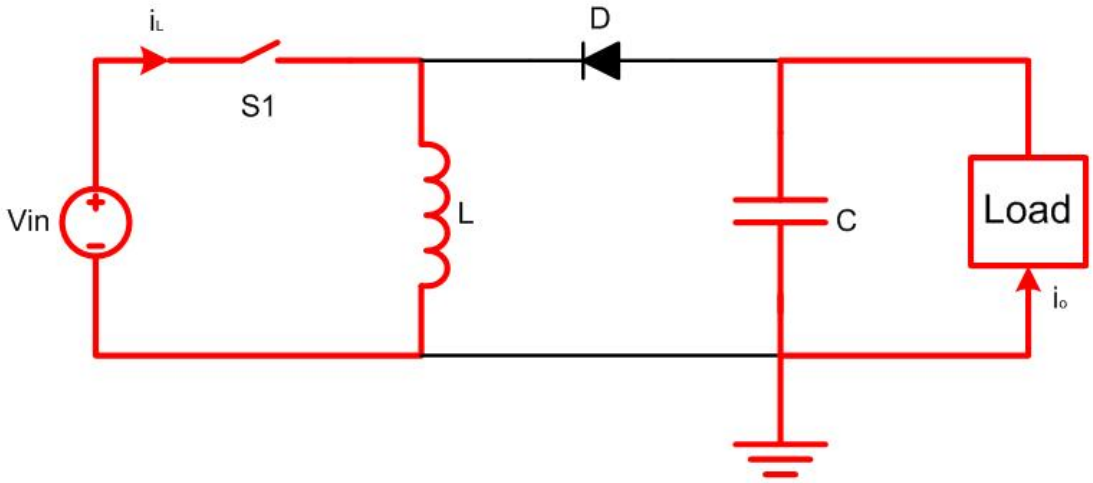

Figure 2.2: Buck-boost mode 1: Switch is ON

Similarly, *mode*2 is defined when the switch is OFF and it is shown in Figure 2.3. By assuming an ideal diode without any voltage drop, as well as a large enough capacitor to remain a constant charge, we can derive eq. (2.3). Because it is known that this time interval is from 0 to $(1 - D)T$ then the equation for i_L can be described as eq. (2.4).

$$\frac{d}{dt} I_L = \frac{V_o(t)}{L} \tag{2.3}$$

$$i_L = \int_0^{(1-D)T} \frac{V_o}{L} dt = \frac{V_o\,(1 - D)\,T}{L} \tag{2.4}$$

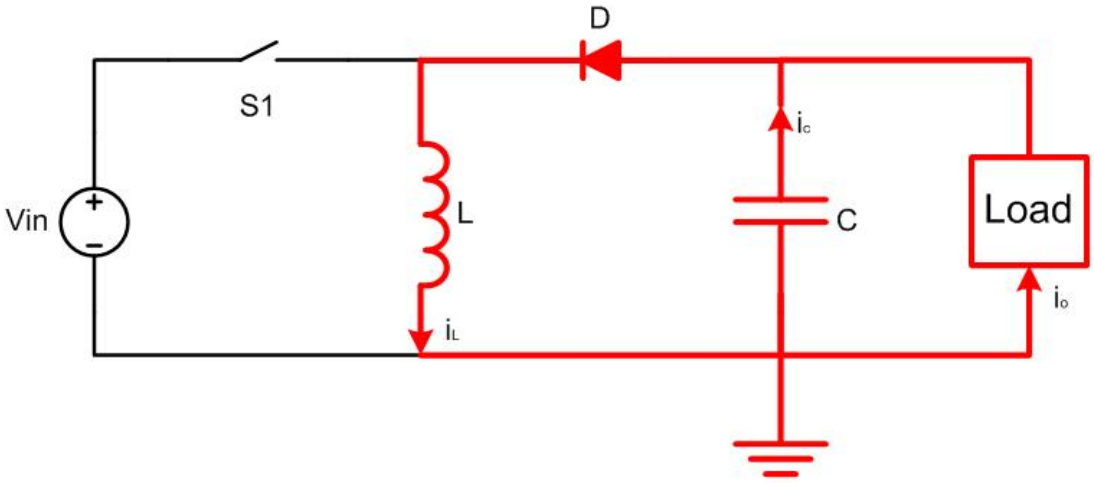

Figure 2.3: Buck-boost mode 2: Switch is OFF

Because we assume that there is steady state operation, eq. (2.5) is used to derive the gain of the converter thus obtaining eq. (2.7).

$$\Delta I_{L_{mode1}} + I_{L_{mode2}} = 0 \tag{2.5}$$

$$\frac{V_{in}DT}{L} + \frac{V_o(t)}{L} = 0 \tag{2.6}$$

$$\frac{V_o}{V_{in}} = -\left(\frac{D}{1-D}\right) \tag{2.7}$$

This converter is considered a basic direct-connected second order converter [Bat04]. However, there are other buck-boost type converters such as the Cuk, SEPIC, and Zeta, for example. These converters are considered as fourth order converters.

In order to figure out a good estimation of the power ratings for the converter, a simulation was done using Orcad Pspice software. This switching model shown in Figure 2.4 assumed a 3 phase input amplitude of 30V each out of phase by 120 degrees similar to the maximum

power specifications of a low power wind turbine. This simulation schematic also contains two extra inductors to filter the input and output of the converter as well as a filter capacitor at the input. These components are of a much smaller scale in compared to the main inductor and the bus capacitor respectively.

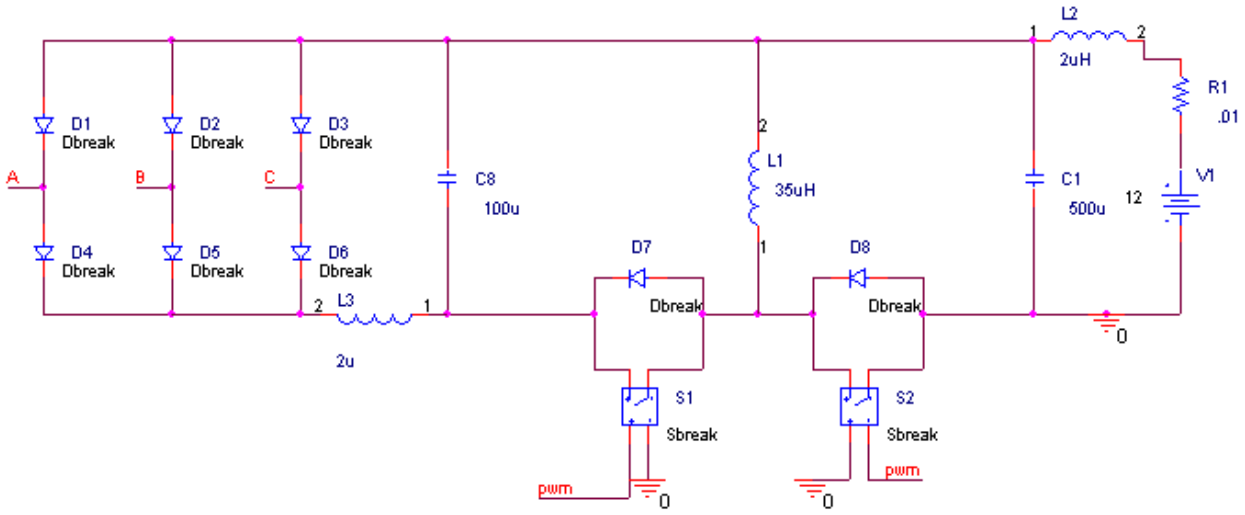

Figure 2.4: Buck-boost schematic using Orcad Pspice

2.1.1 Small signal model for the buck-boost converter

Now that the average model equations have been derived for the buck-boost converter, they can be used in a software program to help verify the results. Once these equations are verified, it will significantly help with the design of the digital controller. The simulation software used for this case was implemented in Matlab Simulink.

Before the average model is developed, a small signal buck-boost schematic was developed and it is shown in Figure 2.5. In this schematic, the switch was replaced by a dependent current source. This current equals to the inductor current when the switch is on. Therefore, when $d = 0$, the current through the switch is zero. By the same token, the diode was replaced by a dependent voltage source. This voltage source is equivalent to the difference between the node voltage, V_g, and the capacitor voltage, V_c, when the switch is on. When the switch is off, the diode is in reverse bias thus blocking the voltage. Assuming this diode is ideal, then the voltage across equals zero.

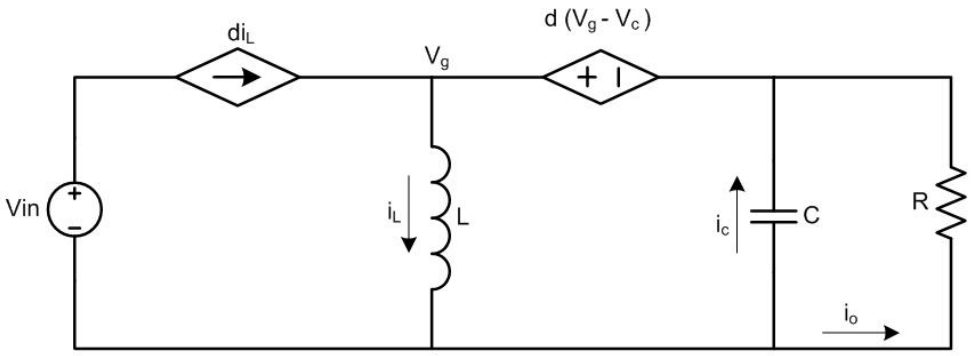

Figure 2.5: Buck-boost small signal schematic

Therefore, we can derive the input current to be eq. (2.8) and the average inductor current to be eq. (2.9). Both of these equations are equivalents to eq. (2.4) derived earlier.

$$i_{in} = D * i_L \tag{2.8}$$

$$i_L = \frac{V_{in}D - V_o(1-D)}{sL} \tag{2.9}$$

We then derive eq. (2.10) and eq. (2.11) to obtain the output current equation shown in eq. (2.12).

$$i_c = i_{diode} - I_o \tag{2.10}$$

$$i_{diode} = (1 - D)\, i_L \tag{2.11}$$

$$I_o = (1 - D)\, i_L - I_o \tag{2.12}$$

These equations are useful to develop an accurate average model for the buck-boost converter. Using Matlab Simulink, the appropriate model was achieved and it is shown in Figure 2.6.

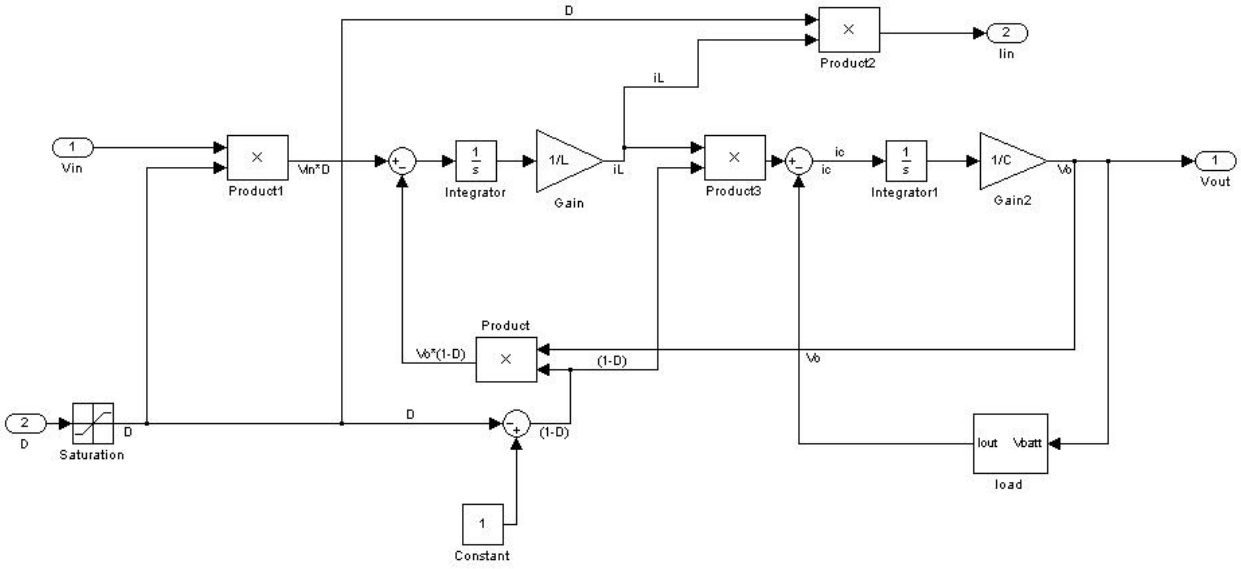

Figure 2.6: Buck-boost small signal schematic

In order to verify the average model shown in Figure 2.6, we used the switching model toolbox known as PLECS in Matlab Simulink. The switching model can be seen in Figure 2.7. This switching model can be used to simulate the controller response of the system. However,

this will consume a lot of simulation time since the time constants of the controller are much larger than the switching frequency. Then, we used PLECS to verify the average model with the switching model.

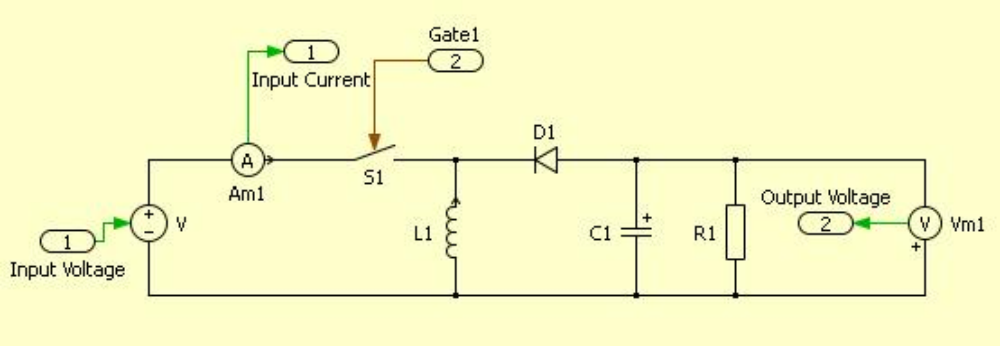

Figure 2.7: Buck-boost converter switching model using PLECS

This switching model was coupled with the average model under the same input conditions. Both output voltage and input current were fed under the same scope and the simulation schematic is shown in Figure 2.8.

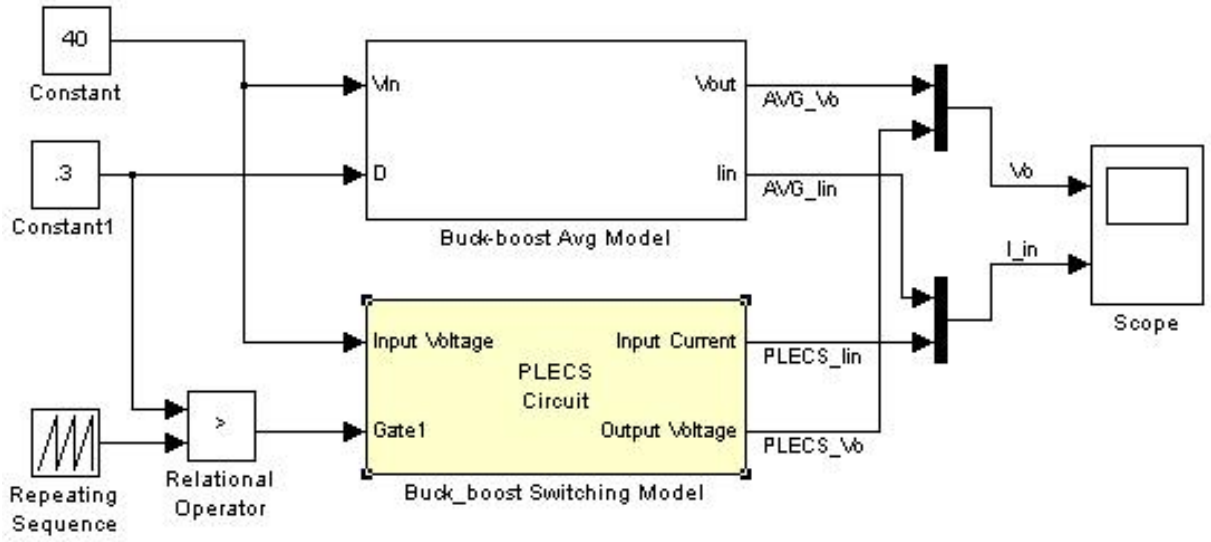

Figure 2.8: Buck-boost average and switching model

It is shown in Figure 2.9 that the average model (in yellow) appears to be the average value of the switching model (in red). The top graph shows the output voltage for both models. If we were to zoom into this graph, we would be able to notice both yellow and red lines are really close to each other. Due to scaling error, this plot appears to be graphing only the switching model. The bottom graph clearly shows both switching and average model. Therefore, we can conclude that the average model derived can accurately predict the behavior of the switching converter.

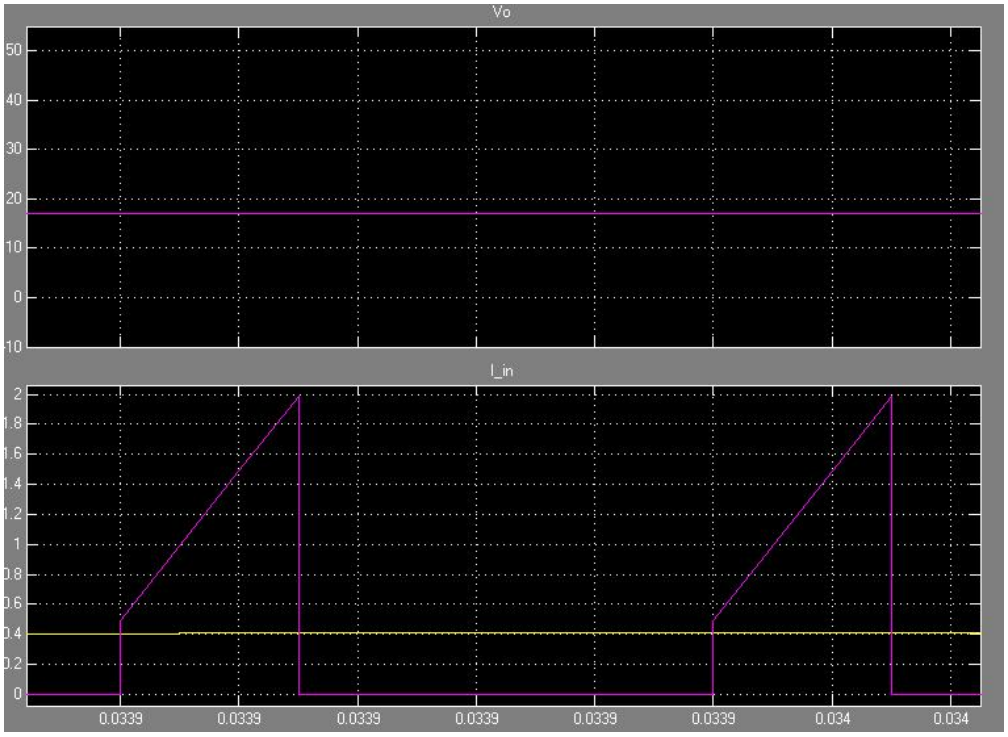

Figure 2.9: Verify simulation small signal model for the buck-boost

2.2 Two stage AC/DC converter: VIENNA rectifier with a Buck Converter

This AC/DC converter consists of a two stage power conversion. The first stage consist of the VIENNA rectifier which is a type of three phase boost rectifier. However, this rectifier uses bidirectional switches which allows sharing of the same high side gate signal. This two stage AC/DC converter shown in Figure 2.10 has a slightly greater component count that the buck-boost converter thus making it slightly more expensive. However, the overall efficiency

is greater than the buck-boost due to power factor correction. Because PFC will be applied to this converter, it requires a higher sensing component count such as input current required for the control algorithm. Initially, the VIENNA rectifier was proposed with the intent to

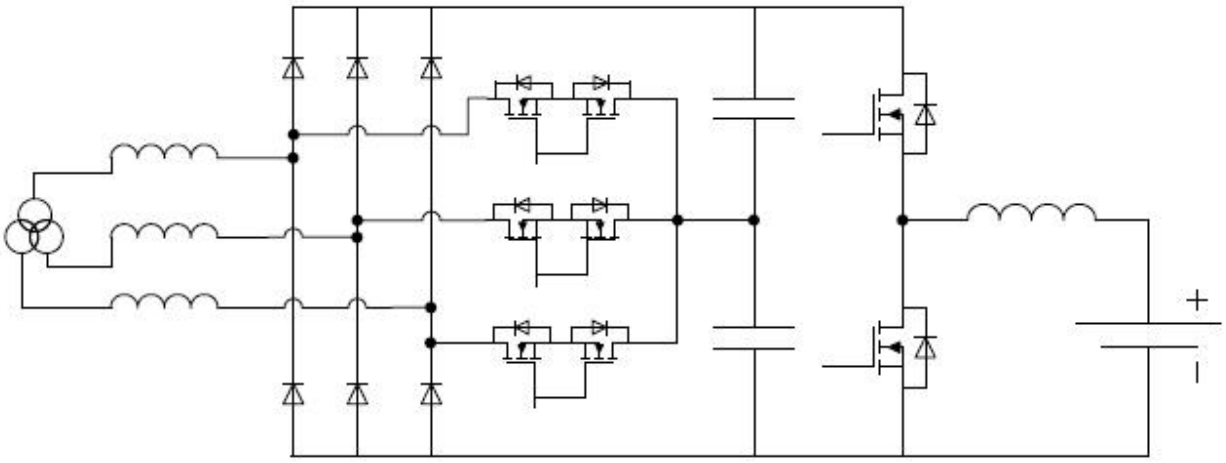

Figure 2.10: Two stage AC/DC converter: VIENNA rectifier with buck converter.

increase the power density of three phase power supplies for telecommunication applications [KZ97][KEZ96]. Due to the advancements in magnetic, power semiconductors, and cooling techniques within the recent years, the VIENNA has kept its great reputation as one of the converters preferred when high power density is desired. Space vector analysis is used in many papers in order to divide the proper control algorithms [BLP07]. The VIENNA converter analyzed in this research can be described as a three phase two stage AC/DC converter where the first stage is a VIENNA rectifier and the second stage is a buck DC/DC converter to better control the battery voltage and develop the proper charging control. The

small signal analysis for this converter is done separately. Each stage is under its own control loop and they can be simulated separately.

2.2.1 Small signal analysis for the VIENNA rectifier

The VIENNA converter is mathematically analyzed in [KA02] [YA07] [YAK06] based on a local linearization around the nominal operating point of the differential equation non-linear averaged model using the following techniques:

- Averaging technique to system
- Frame transformation matrix K (known as Park's transformation matrix)

However, due to simplicity of analysis, the derivation of the small signal analysis described in this research is slightly different than the analysis described in [KA02] [YA07] [YAK06]. The VIENNA rectifier, shown in Figure 2.11, is has a sinusoidal input voltage thus taking a positive voltage in one half of the AC cycle and negative voltage at the other half cycle. If only one phase is considered in the analysis, as shown in Figure 2.12, it can simplify the analysis of the small signal model. To simplify even further, when only the positive cycle is considered, the topology will then become a boost converter as shown in Figure 2.13. Therefore, if the small signal analysis is applied to the boost converter, it can then be reverted back to the VIENNA rectifier in a much simpler manner. This small signal analysis, just like the buck-boost described in section 2.1.1, will help develop an average model in Matlab Simulink in

order to verify the controls. The drawback of this simplified small signal analysis is that

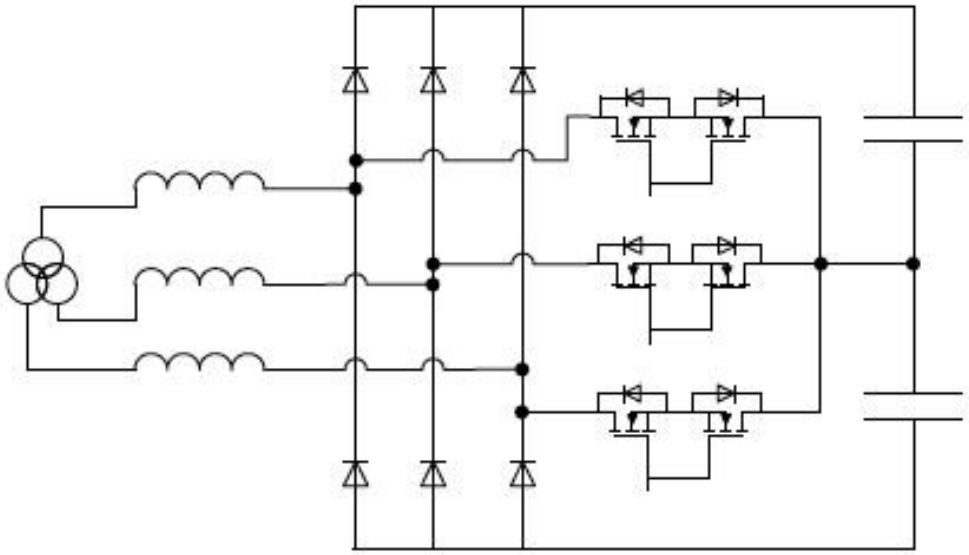

Figure 2.11: VIENNA Rectifier.

it requires numerous assumptions. For a more advanced model of the VIENNA rectifier, mathematical analysis is done in [KA02] [YA07] [YAK06] which might be a more accurate model. This model is used to verify the design of the digital control loops. Therefore, the simplified small signal model will be sufficient for this research. The assumptions in this average model are:

- No switching or conduction power loss
- Power pushed in the positive cycle equals the power pushed in the negative cycle
- The total bus voltage equals exactly twice the value of each individual capacitor voltage
- Each input phase are exactly 120 degrees off phase from each other

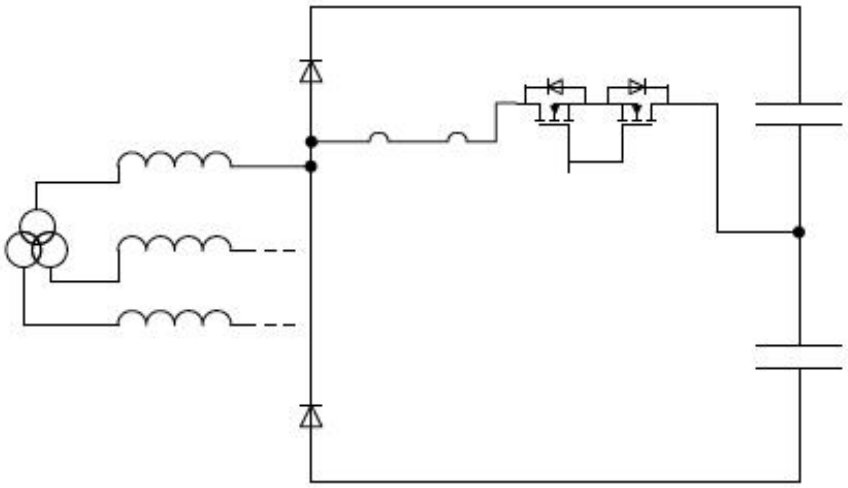

Figure 2.12: VIENNA Rectifier (One Phase).

- All three phases provide the same amount of power

2.2.1.1 Boost Model Analysis

In the boost converter, shown in Figure 2.14, the output voltage is higher than the input voltage. Similar to the buck-boost analyzed in section 2.1, this converter can be divided into two operating modes.

- $Mode1$ is defined when the converter switch is closed. This period of time is known to be from 0 to DT.
- $Mode2$ is defined when the converter switch is open. Similarly, this period of time is known to be from DT to T (also known as 0 to $(1-D)T$).

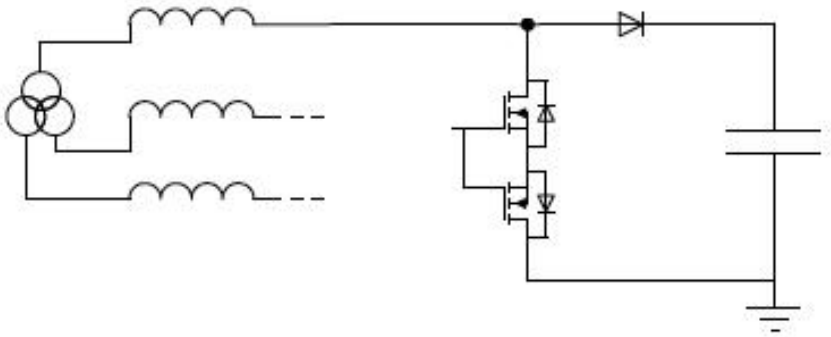

Figure 2.13: VIENNA Rectifier (One Phase Positive Cycle).

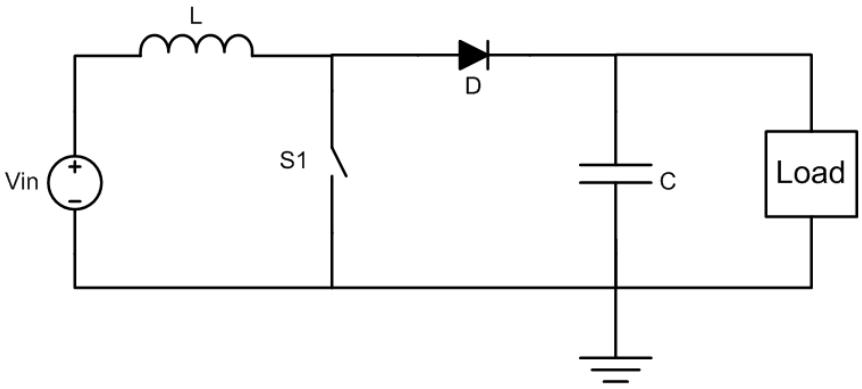

Figure 2.14: Boost converter

For the purpose of the VIENNA analysis, this converter is be on the positive half cycle of the sinusoidal input voltage, thus behaving as a variable positive input voltage. In *mode*1, shown in Figure 2.15, the input is directly connected to the inductor, therefore supplying current and accumulating energy. In this mode, the capacitor is disconnected from the input and it alone supplies current to the resistive load. This equation is similar to the one derived for the buck-boost converter. When solving for i_L throughout the time interval 0 to DT,

eq. (2.13) is derived. In this equation, $I_L(0)$ is defined as the initial inductor current that corresponds to the minimum inductor current value.

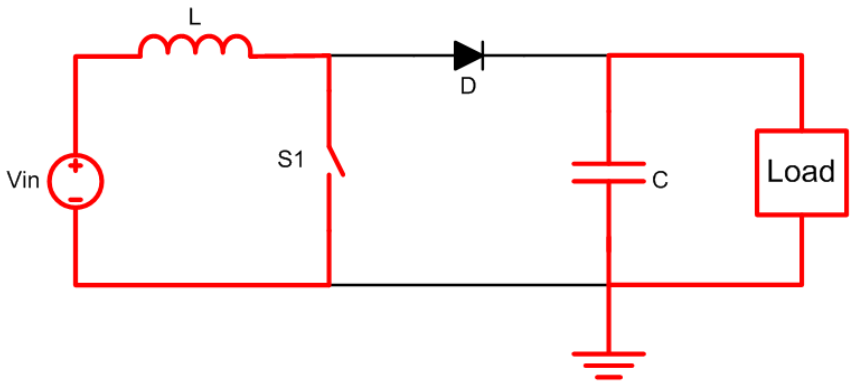

Figure 2.15: Boost mode 1: Switch is ON

$$i_L = \frac{V_{in}(t)}{L} + I_L(0) \tag{2.13}$$

$Mode2$, defined when the switch is OFF from DT to T, is shown in Figure 2.16. Unlike the buck-boost, the input is not disconnected from the output. By assuming an ideal diode without any voltage drop, we can derive eq. (2.14).

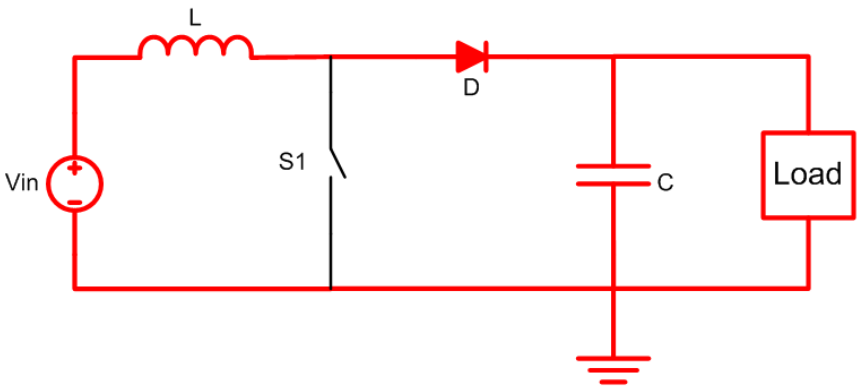

Figure 2.16: Boost mode 1: Switch is ON

$$i_L = \frac{1}{L}\left(V_{in} - V_o\right)\left(t - DT\right) + I_L(DT) \tag{2.14}$$

If we use the fact that $I_L(T)$=$I_L(0)$, then we can set eq. (2.13) and eq. (2.14) equal to each other and solve for the voltage gain of the converter shown in eq. (2.15).

$$\frac{V_o}{V_{in}} = \frac{1}{1 - D} \tag{2.15}$$

2.2.1.2 Modification on the boost to fit the VIENNA model

Once the analysis for the boost converter was completed, the next challenge was to modify such model to make it behave like a VIENNA rectifier. The first observation was that in the VIENNA rectifier, only one capacitor is charged at a time for a single phase topology. The top capacitor is charged during the positive cycle and the bottom during the negative cycle. Never do these capacitors charge on a same charging phase (assuming ideal switching). Thus

the charging mode for each output capacitors must be switched accordingly. Therefore, to model this behavior correctly in the average model, two extra switches were introduced into the model in order to control the path of each phase cycle. The model for a single phase VIENNA is shown in Figure 2.17.

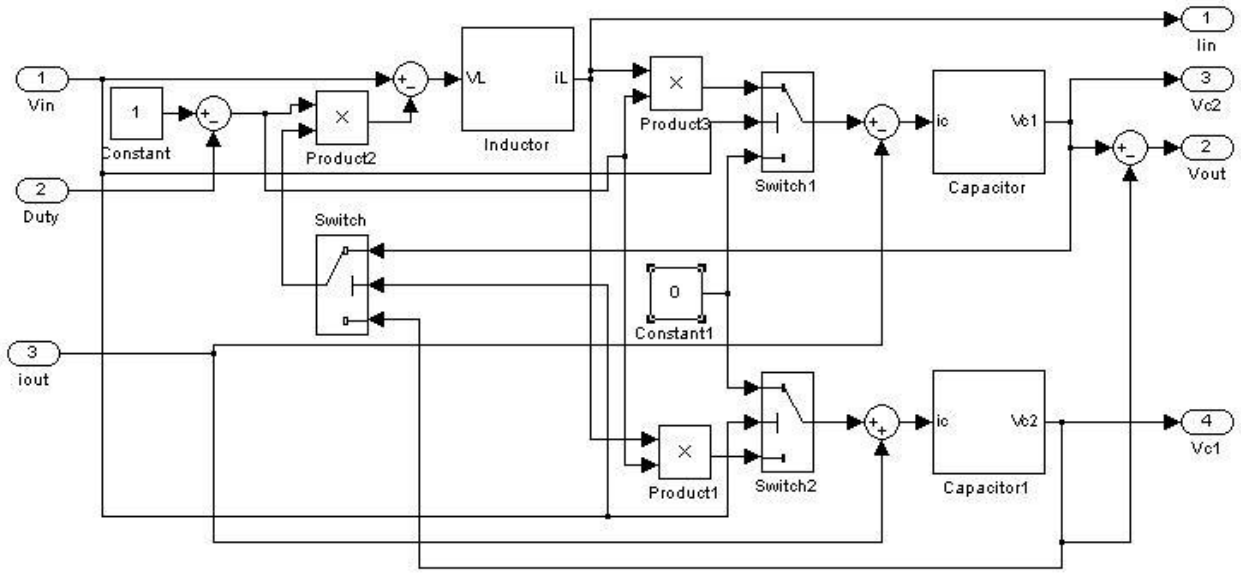

Figure 2.17: VIENNA Rectifier Model (Single Phase)

The inclusion of two switches, Switch1 and Switch2, helped model the usage of each capacitor charging time in a complementary manner. In other words, when the input voltage V_{in} is on the positive cycle, the input inductor will charge the top output capacitor C_1. Similarly, when V_{in} is on the negative cycle, the input inductor will charge the bottom capacitor C_2. Each switch reads the input voltage and reacts depending on whether the signal is positive or negative. For example, if we only consider looking at Switch1, when the input voltage is positive, the capacitor C_1 is charged due to the current input inductor.

However, when the input voltage is negative, it blocks the signal and it sends a constant zero amps thus preventing the capacitor from being able to charge anymore. During this period, the top capacitor slowly discharges because it gets some feedback from the overall output current. Similarly, Switch2 is in charge of only letting the input inductor current pass when the phase is negative, charging only the bottom capacitor, C_2. Extra precaution was taken with the negative phase charging since polarities are reversed. A few multiplication boxes were added in order to multiply by +1 or -1 accordingly. After successfully modeling a single phase for a VIENNA rectifier, Figure 2.18 illustrates how the concept was implemented for all three of the phases.

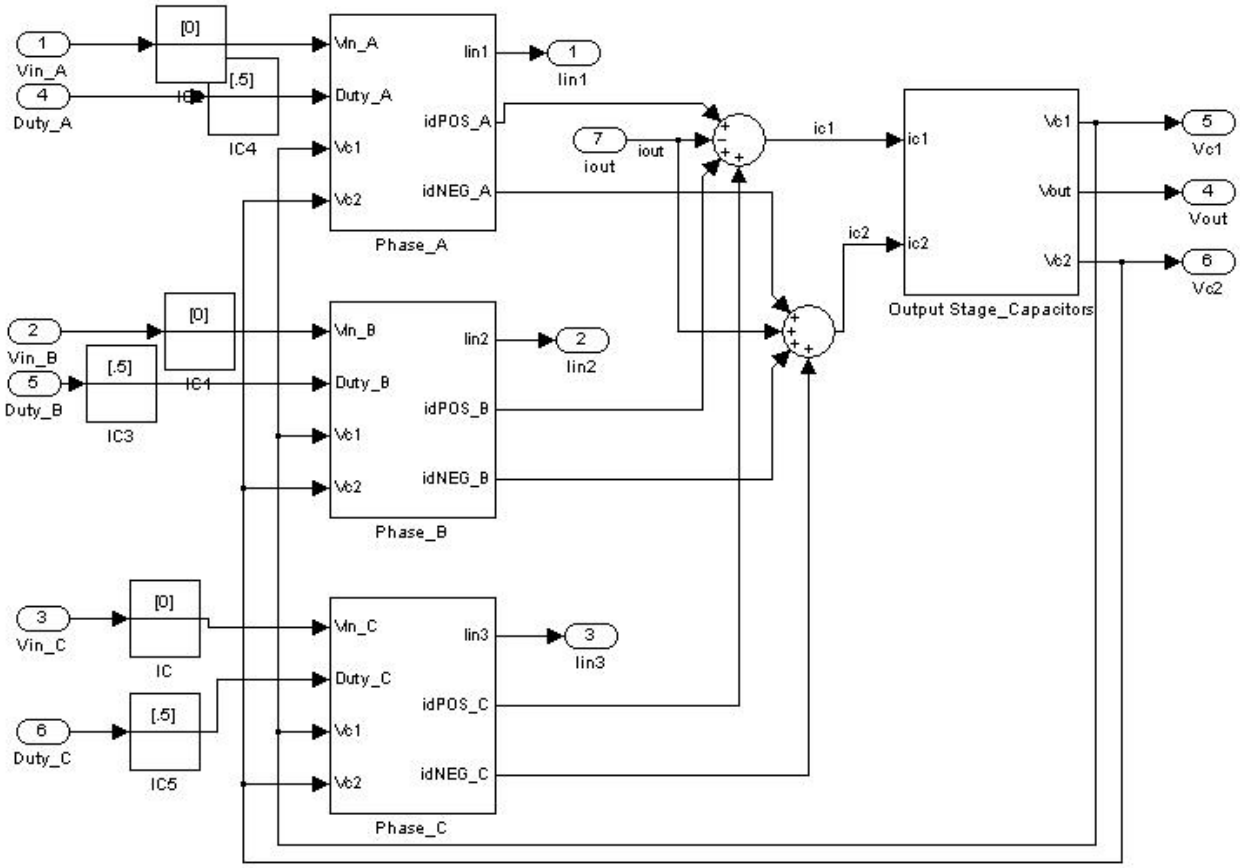

Figure 2.18: VIENNA rectifier model (Three Phase)

Because the three phase input will vary in amplitude, this model was tested with a simulation subsystem that behaves similar to a wind turbine. This model, shown in Figure 2.19, takes into consideration the current drawn from the turbine and changes its characteristics properly. For example, when the output of the wind turbine draws high current, the turbine phase voltage will decrease in amplitude as the current increases. This causes the wind turbine to slow down which decreases its frequency.

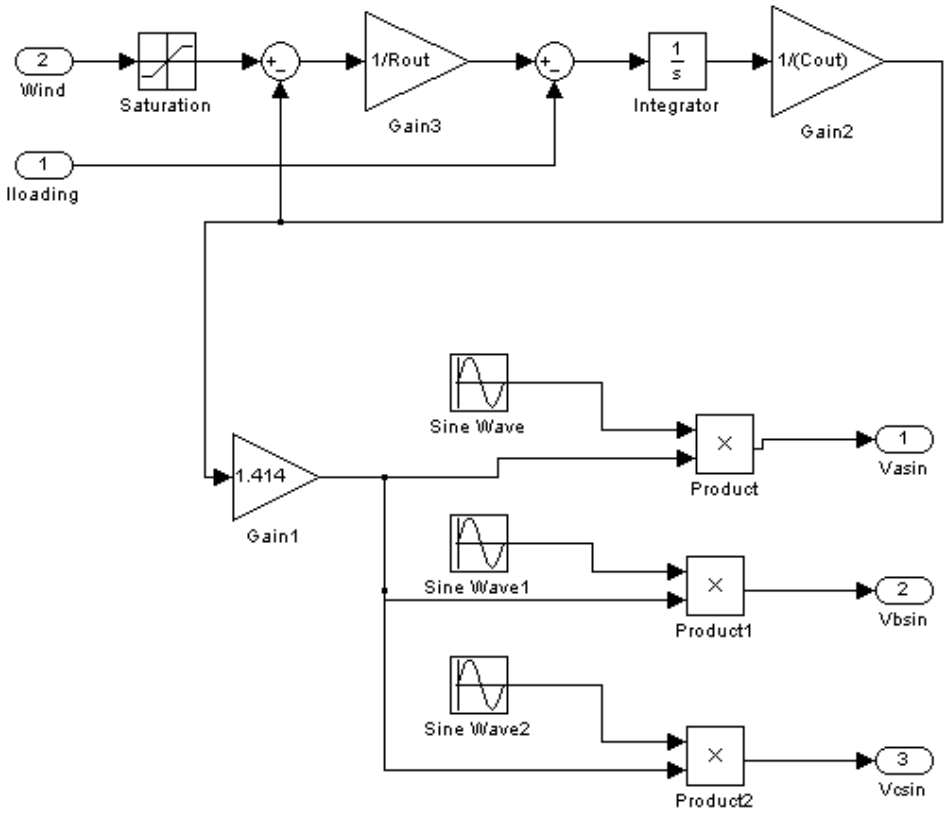

Figure 2.19: Wind turbine model used in the VIENNA rectifier simulation

However, due to simplicity in the model, this model does change its frequency depending on the loading. This simplification was implemented because simulation time was slow. This assumption helped the program simulate the converter much quicker. Therefore, the model first calculates an RMS voltage depending on the given wind speed profile. This RMS value will be sent to each individual phase which will then be multiplied by a unity amplitude phase input. Each input is 120 degrees out of phase thus originating a three phase input at the

RMS amplitude voltage. Using a fixed frequency of 20Hz, this wind turbine model was used as the input of the VIENNA rectifier model. The output voltage is shown in Figure 2.20.

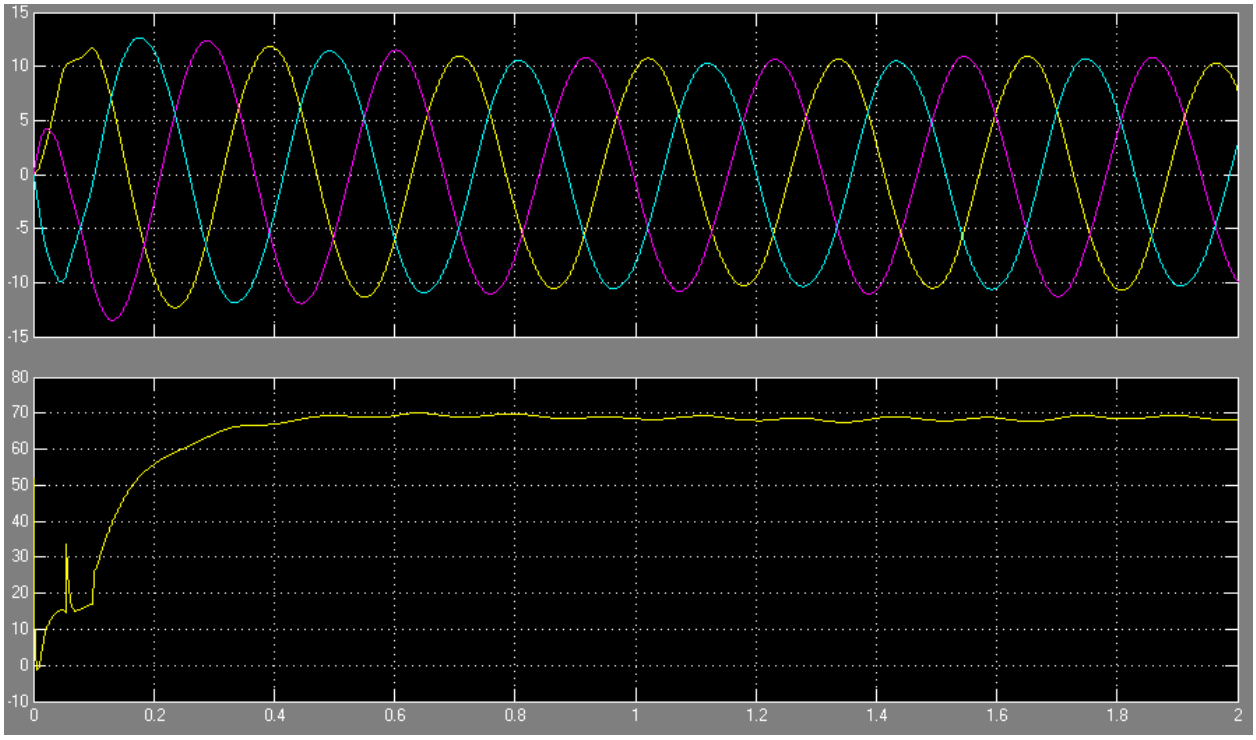

Figure 2.20: VIENNA rectifier simulation results: Input phase voltage (top), rectified output voltage (bottom)

2.3 Part Selection

For any power electronics converter, it is important make the appropriate trade-offs between all the power losses and overall cost. This section will describe some of the main components

where most of the power loss might be concentrated. If these devices are carefully designed, it can make a major improvement in the efficiency at a low cost. The topics discussed are:

- Switching device: power MOSFET selection.
- Rectifying device: 3 phase schottky rectifier selection.
- Sensing device: current and voltage amplifier design.
- Cost summary.

2.3.1 Power MOSFET

Because the converter is designed to charge a battery at a 300 watts typical as well as being able to withstand a peak power up to 900 watts for a short period of time. Therefore, at 900 watts, the switching transistor for the buck-boost converter must handle current flow of up to 75A when charging a 12V battery. On the other hand, not all the MOSFET for the VIENNA need to be able to handle that much current. Only the second stage MOSFETs of the converter need to handle approximately 75A. The other switching transistors are located in the first stage and their current rating will depend on the maximum power of the wind turbine. For a 200W turbine, the current flowing through these devices might not excede 15A. It is obvious to note that this value increases as the maximum power of the turbine increases as well.

To obtain the best efficiency, several tradeoffs in the MOSFET characteristics must be carefully analyzed. On-resistance and switching loss are two of the dominant factors in the total power loss for power electronics converters as their switching frequencies being increased to reduce the size of passive components [JXC06]. This subsection will analyze physical characteristics of the power MOSFET and several components will be investigated and tested and the best MOSFET will be picked that offers a low power loss and cost. The performance of a power MOSFET is restricted by the internal resistance and it is useful to pick a structure that ascertain the minimum valueand that is capable of supporting the desire blocking voltage [Bal08]. The On-resistance consists of several factors as shown in eq. (2.16).

$$R_{DS(on)} = R_{source} + R_{ch} + R_A + R_J + R_D + R_{sub} + R_{wcml} \tag{2.16}$$

Where R_{source} is the source diffusion resistance, R_{ch} is the channel resistance, R_A is the accumulation resistance, R_J is the $''JFET''$ component resistance between the two body regions, R_D is the drift region resistance, R_{sub} is the substrate resistance and R_{wcml} is the sum of the Bond Wire resistance; the contact resistance between the source and drain Metallization and the silicon metallization and Lead frame contributors [Bar]. This resistance is negligible for high voltage applications; however, it can be significant in low voltage applications. These resistance is illustrated in a power MOSFET structure in Figure 2.21. We must also take into consideration that the on-resistance of a power MOSFET increases rapidly with the device blocking voltage because of increased drift region resistance[Che05].

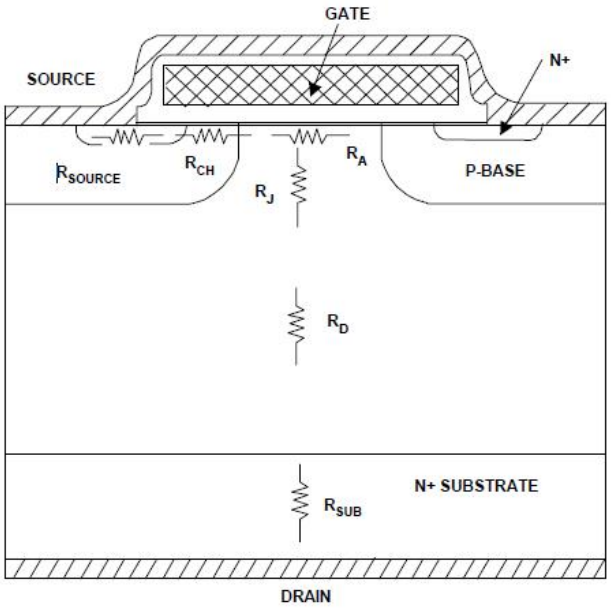

Figure 2.21: On-resistance in a power MOSFET structure[Bar]

A list of power MOSFETS that were considered for the buck-boost design and the second stage (buck stage) of the VIENNA converter are listed in table 2.1. Notice that as the drain current handling capability increases, the on-resistance lowers. The lower the on-resistance the better, but it increases losses in other areas such as switching.

Table 2.1: MOSFETs considerations

Part Number	$R_{DS_{(on)}}$ (typ.,max.)	I_D (A)	V_{DSS} (V)
IRFP1405PbF	4.2mΩ, 5.3mΩ	95	55
IRFP064VPbF	- , 5.5mΩ	130	60
IRFP4410ZPbF	7.2mΩ, 9.0mΩ	97	100
IRFP4110PbF	3.7mΩ, 4.5mΩ	120	100
IRFP4310ZPbF	4.8mΩ, 6.0mΩ	120	100
IRFP4468PbF	2.0mΩ, 2.6mΩ	195	100

As described earlier, switching loss can be very significant in the overall power loss of the power MOSFET. Complex switching behaviors and power losses are difficult to model analytically because the parasitic capacitance and the inductive load of power electronic converters for a power MOSFET is highly non-linear. A commonly used formula for estimating the power MOSFET drain to source switching loss is shown in eq. (2.17).

$$P_{SW} = \frac{1}{2} I_D V_D \left(t_{off} + t_{on}\right) f + \frac{1}{2} C_{oss} V_D^2 f \tag{2.17}$$

Assuming that there is a linear transition between the on-off process, the first term of the eq. (2.17) simply calculates the power loss as the area of the below I_D and V_D at the transition periods in Figure 2.22, and the second term is often referred to as the output capacitance loss [JXC06].

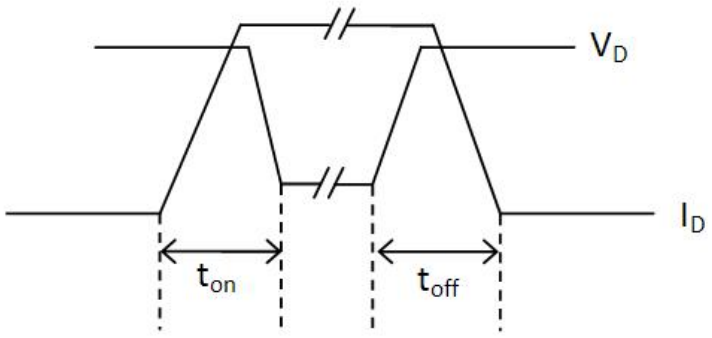

Figure 2.22: Switching waveform of a power MOSFET

C_{OSS} is known as the output capacitance of the power MOSFET and is derived by eq. (2.18). The switching times are often estimated by eq. (2.19).

$$C_{OSS} = C_{GD} + C_{DS} \tag{2.18}$$

$$t_{on} = t_{off} = \frac{Q_{sw}}{I_G} \tag{2.19}$$

Where the Q_{sw} value can be obtained from the power MOSFETs datasheet and its known as the gate switch charge. I_G is the gate drive current and it is also provided on datasheets. Although, in paper [JXC06] explains how these equations are widely used in technical articles, textbooks and technical notes, it is to very accurate since it assumes a highly linear approximations of V_DS, this equation will be used in this paper to approximate switching losses from the information given on power MOSFETs datasheets.

Using eq. (2.17), table 2.2 is originated. One of the assumptions made in this table is the time it takes the MOSFET to turn on and off. For simplicity of the analysis, we assume t_{on} to be the same as t_{off}.

Table 2.2: MOSFETs switching loss approximation: $I_D = 20A$, $V_D = 40V$, $f_{sw} = 100kHz$, $I_G = 2A$

Part Number	C_{OSS} (pF)	$Q_{sw}typ.$ (nC)	$t_{on} = t_{off}$ (nanoseconds)	P_{sw} (W)
IRFP1405PbF	1310	120	60	4.905
IRFP064VPbF	1330	260	130	10.506
IRFP4410ZPbF	340	83	41.5	3.347
IRFP4110PbF	670	150	75	6.054
IRFP4310ZPbF	490	120	60	4.839
IRFP4468PbF	360	360	180	14.509

Table 2.2 also assumes a constant gate current of 2A. Using ohms law, shown in eq. (2.20), this gate current highly depends on the gate resistor value that is picked since the gate voltage is typically 10V. The drain to source voltage stress of the MOSFET is assumed to be 40V. After various simulations and testing, this value is a good approximation of the average voltage stress of the switch.

$$I = \frac{V}{R} \tag{2.20}$$

A linear relationship of the power loss due to switching for each power MOSFETs were plotted in Figure 2.23 in terms of the drain current of the device. This plot allows us to trade off the power losses and pick a device that best fits the power specification of the converter. Notice that from .1 to 10 amps, $IRFP4410$, $IRFP4310$, and $IRFP4110$ have

very similar switching losses while having very distinct on-resistance range (see table 2.2). $IRFP4468$ appears to have the lowest on-resistance, however, notice that the switching loss is much higher than the rest of the device. Because each line has a different slope, the difference between the switching power losses of the drain current higher than 10A becomes very significant. Knowing that the increase in on resistance decreases switching loss, this figure helps illustrate this effect. Remember that this is an estimation of the power loss; the actual power loss is a non-linear relationship.

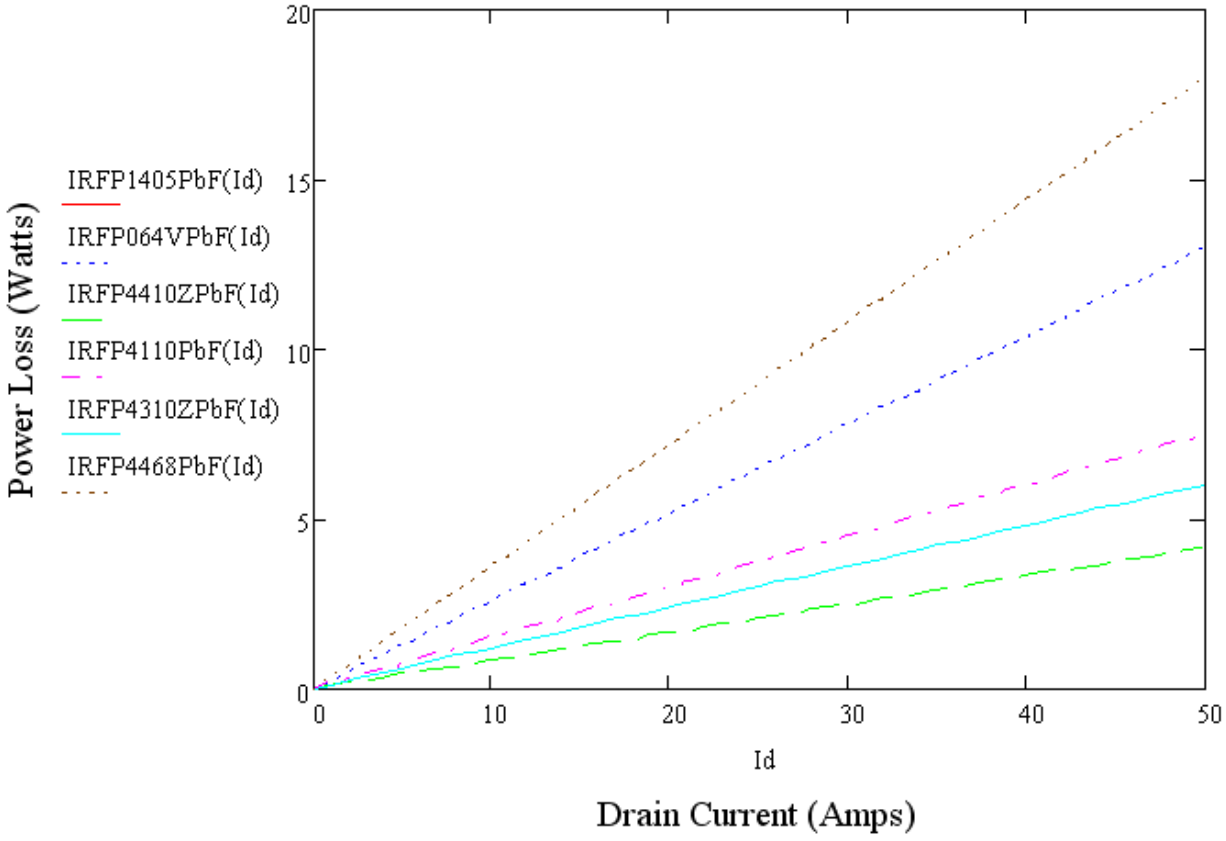

Figure 2.23: Switching power loss vs. drain current: $V_D = 20V$

The LM5101AM is a high voltage gate driver that is designed to drive both high side and low side of the N-channel MOSFET for both the buck-boost and the VIENNA. The VIENNA will utilize this driver on its second stage. This gate driver will be able to provide a full 3A gate drive.

2.3.2 Rectifying diode selection

Because the three phase input of the buck-boost will be rectified, finding the best power diode that offers fast reverse recovery with a low on-state voltage drop and high blocking voltage, will significantly improve the overall efficiency of the converter. For our application, schottky diodes are used because they offer fast switching speed but also to eliminate the large reverse recovery current observed in high voltage silicon P-i-N rectifiers. Also, the much lower resistance of the drift region for silicon carbide enables the development of such shottky rectifiers with high breakdown voltage[Bal08].

The simulation profile shown earlier in Figure 2.4 is used to estimate the voltage stress across the rectifying diodes. These diodes are assumed to be ideal since we are only trying to find the stress of the diode under maximum conditions. The simulation result of the voltage stress of diode $D1$ is shown in Figure 2.24. The peak to peak voltage stress of the individual diode appears to be around $\pm 16V$ to $\pm 18V$ at 30V input amplitude phase voltage. Similarly, it is important to know the maximum current the converter will be operating at and to make

sure that these diodes are capable of handling these power ratings. The current across the inductor was plotted shown in Figure 2.25.

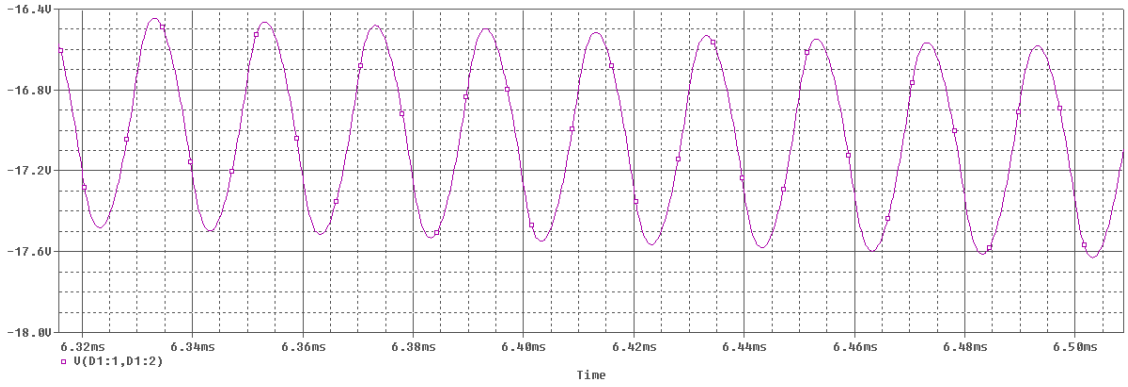

Figure 2.24: Buck-boost diode $D1$ voltage stress with a input voltage amplitude of 30V

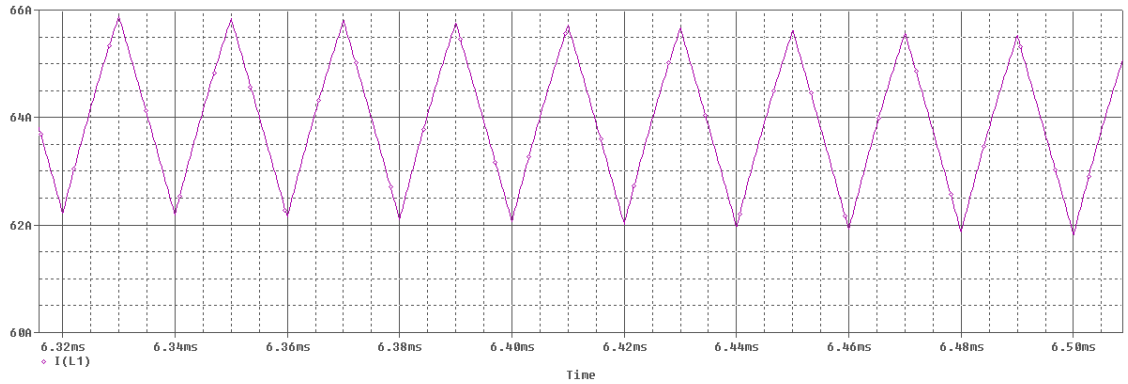

Figure 2.25: Buck-boost inductor current with a input voltage amplitude of 30V

2.3.3 Sensing

There are several methods for sensing current and voltages in a power converter. However, the use of a seining amplifier is one on the methods adopted by many design engineers due

to its low cost, high reliability and simplicity of the design. This signal will then be sent to an analog to digital controller (ADC) that is built-in to the DSP controller.

To monitor the current going into the battery, a sense resistor was added closed to the output terminal of the converter. The voltage drop across the sense resistor is captured by the by an amplifier design and calculates the current flow. Appropriate scaling is applied in order mainly because the output of the amplifier will be sent to the digital to analog converter (DAC) of the microcontroller which will require a value from 0 to 5V; where 0 represents the minimum amount of current and 5V the maximum current of the converter. A schematic of this sense amplifier is shown in Figure 2.26. R_{27} determines the input impedance of the amplifier circuit while R_{24} along with the pull down resistor R_{38} provides a voltage offset. When the sense current goes to a negative value, this DC offset used to fix this issue. Because the microcontroller can only take voltage from 0 to 5V, negative voltage is undesirable. Also, the op-amp V_{cc} negative terminals are grounded. This means that the minimum output voltage the op-amp can provide is zero volts. Therefore, it will become impossible to properly measure negative voltage (meaning voltage flowing away from the battery) across the sense resistor. A highly regulated 5V is used to supply power this op-amp. In the same manner, this 5V supply is also sent to the voltage divider. Using eq. (2.21), R_{24} is picked so that it can provide the proper DC offset. The value for the feedback resistor is picked so that it will match the input impedance of the circuit.

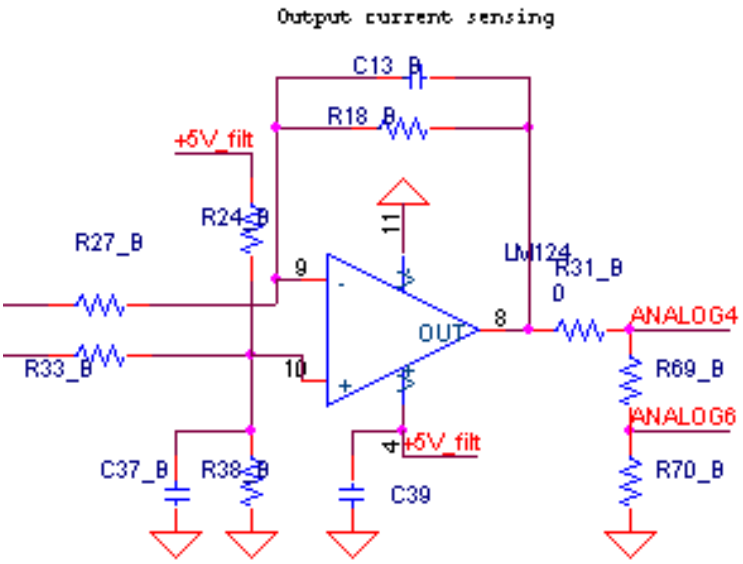

Figure 2.26: Buck-boost current sense amplifier circuit

$$V_{DC_{offset}} = \frac{R_{38}}{R_{38} + R_{24}} V_{5V_{filtered}} \tag{2.21}$$

The scaling of the amplifier can be realized by knowing the maximum voltage or current that is being sensed. Assuming that the maximum voltage is 60V, for example, then eq. (2.22) can be applied where A_v is the voltage gain defined as V_o/Vin and we let $R_a = R_{27} = R_{33}$ and $R_b = R_{38} = R_{18}$ as shown in Figure 2.26.

$$A_v = \frac{R_b}{R_a} \tag{2.22}$$

Therefore, we can re-write eq. (2.22) by knowing that the maximum output voltage from the microcontroller will be 5V when sensing an input voltage of 60V. If we assume R_{27} to be 120kΩ, then we can re-arrange eq. (2.23) and obtain eq. (2.24). Different voltage gains can

be considered for a current sense case since this is just an example for measuring a peak of 60V.

$$\frac{5V}{60V} = \frac{R_{18}}{120k\Omega} \tag{2.23}$$

$$R_{18} = 120k\Omega \times \frac{5V}{60V} = 10k\Omega \tag{2.24}$$

2.3.4 Cost summary

The low component count of the buck-boost converter gives a great advantage over the VIENNA because it introduces a much lower converter cost. However, efficiency also plays a big roll when choosing a converter. If the efficiency difference between the converters that are being considered is not great, then the designer can trade a little efficiency for a big cost reduction. Therefore, it is important to track the cost of each of the converter that are being considered. An estimated cost analysis for the buck-boost converter design is summarized on table 2.3.

Table 2.3: Buck-boost converter cost summary

Description	Count (per converter)	Price (total) ($ per 100k units)
Power MOSFETS	2	1.05 (2.10)
Schottky diodes	6	0.20 (1.20)
Bus capacitors	2	0.10 (0.20)
Inductor(s)	1	0.50 (0.50)
Power supply	1	2.00 (2.00)
Driver(s)	1	1.40 (1.40)
Sensing	3	0.40 (1.20)
DSP board	1	3.00 (3.00)
Miscellaneous	-	6.00 (6.00)
Total		**17.60**

All of these values are approximations at high quantity productions and some prices may vary. The buck-boost converter is costing close to $15 per converter for 100,000 units per year. Note that the miscellaneous items listed above includes an approximated total cost of all the small necessary components such as heat sink, fuse, connectors, filter inductors, and surface mount resistors and capacitors. The sensing includes the input and output voltage measurements as well as the output current. A Quad amplifier chip is used and because only three amplifiers are needed, three of the pins will not be used.

For the VIENNA rectifier with a buck, the cost summary is shown on table 2.4. Unlike the buck-boost, the converter requires more components for sensing, switching, and bus capacitance. Each of the phases uses two power MOSFET that are connected together through the source and sharing the same gate. This type of configuration is called bidirectional switching where current flow is blocked in both directions when the power MOSFET is in the OFF mode. Another advantage of this bidirectional switch is that it shares current stress thus requiring a lower rated device. Each of the phases contains its own set of capacitors which add to the total bus capacitance. Also, two more capacitor were added across the entire bus. This configuration allows the usage of smaller capacitors since this converter also requires a large capacitance at the output in order to be able to hold the charge the first stage is supplying to the second stage.

Table 2.4: VIENNA rectifier with buck converter cost summary

Description	Count (per converter)	Price (total) ($ per 100k units)
Power MOSFETS	8	1.05 and 0.80 (6.90)
Schottky diodes	6	0.15 (0.90)
Bus capacitors	8	0.10 (0.80)
Inductor(s)	4	0.50 (2.00)
Power supply	1	1.20 (1.20)
Driver(s)	4	0.60 (2.40)
Sensing	9	0.32 (0.64)
DSP board	1	3.00 (3.00)
Miscellaneous	-	6.00 (6.00)
Total		**23.84**

Although the approximated price per converter is slightly greater than the buck-boost design, it is important to understand the effect (if any) of power factor correction. If an increase in efficiency is observed, the next step would be to decide whether is worth it or not spend the extra money for the amount of efficiency increase. This VIENNA converter also has the potential to increase reliability of the system due to the implementation of power factor correction. Making the converter look like a purely resistive load to the turbine, it reduces the harmonic distortion as well as the conduction losses. Efficiency results between

these two converters are shown in section 6.4. We must take under consideration that some components could be taken out of the converter and still have the same functionallity. One example is by taking out the user interface of the converter with the computer, the DSP board cost will redurce significantly. These cost are estimates as they may vary depending on how advanced you want the converter to be.

2.4 Topology research summary

Each of these topologies are unique in their own way. Although power factor correction is not implemented on the buck-boost converter, it offers a low component count thus reducing the overall cost. On the other hand, the introduction of power factor may significantly increase mechanical and electrical efficiency. The downside of the VIENNA is that it has high sensing effort techniques. In order to apply power factor correction, the current and voltage for each of the three phases must be sensed. Other sensing components are needed to measure bus voltage and battery current and voltage as well. Therefore, the main characteristics of each converter were analyzed individually to understand the effect of PFC in wind turbine converters.

Table 2.5 introduces a comparison of some of the characteristics of each converter that is going to be analyzed. It illustrates a side-by-side comparison of the buck-boost converter with the VIENNA converter for the same application. Notice the typical operating power each converter must sustain is 300W. One of the main differences between these converters

is the amount of switches needed. The buck-boost converter only requires two synchronous switches and six rectifying diodes on the input. On the other hand, the VIENNA converter requires three bidirectional switches and the six diodes. These bidirectional configurations consist of two switches. For a MOSFET, both devices share the same switching node, connecting their source pins to each other as well as sharing the same gate signal. This means that the VIENNA is utilizing eight switching devices (six in the first stage and two in the second stage).

Table 2.5: Summary of the main topologies researched

	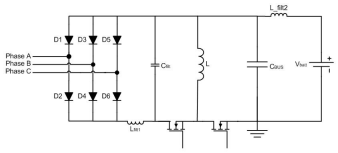	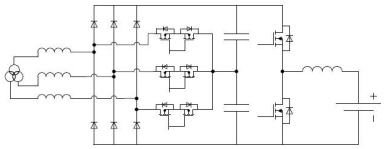
Typical operating power (W)	300	300
Switches	2	8
Diodes	6	6
Maximum bus voltage (V)	30	75
Avg. Efficiency (%) at 50kHz	85	91
Sensing effort	Low	High
Control complexity	Low	High
Cost	Low	Low/medium

Bidirectional switching is used for various application techniques. It allows the topology to block the current flow in both directions as well as a dynamic change in current direction. Topologies such as a VIENNA rectifier, bidirectional switches are used in order to block current flow in both directions when the switch is off. This converter acts like a boost converter that can operate in both positive and negative cycles. More of this topology will be explained in later sections. There are also applications that require current to flow in different directions such as some battery charging converters. Current must flow towards the battery in order to charge the unit. However, when the battery is fully charged, then the current must flow away from the battery. The bus voltage for the buck-boost converter is limited to the maximum RMS voltage the turbine can supply. In other words, this voltage highly depends on the amount of wind as well as the mechanical specifications of the turbine model unless necessary controls are included. For maximum power, the digital controller will find an optimal input value where maximum power can be achieved. After some preliminary results, a maximum input of 30V is assumed. The bus voltage for the VIENNA converter will be less dependent on the amount of wind received since it will boost the voltage to a regulated value no matter what the input voltage is. Bus voltage regulation is included in the controls for this converter which will keep a typical value of 35V-45V. However, when the second stage does not require any more power from the bus, this value will start to increase predominately because the turbine might still be transferring power. For converter protection, the controller will never let this bus voltage reach any higher than 75V. There is also a significant efficiency difference between the two converters. The main goal when designing

the buck-boost converter was to keep the cost as low as possible. In the VIENNA converter, the main goal was to implement power factor correction thus increasing the efficiency at the lowest possible cost per unit.

CHAPTER 3: POWER FACTOR CORRECTION

Power Factor Correction (PFC) is simply the ratio of real power to apparent power as shown in eq. (3.1). The main difference between real and apparent power is that real power is the capacity of a circuit performing for a given time. On the other hand, apparent power is the product of the current and the voltage of the circuit. In other words, real power is the average power of the instantaneous product of voltage and current over a cycle. Apparent power is the the multiplication of the RMS current and the RMS voltage. In many cases, the apparent power can be greater than the real power due to nonlinear loads or stored energy in the load that feeds back into the source that can distort the wave shape of the current drawn from the sources. If a system has low power factor, the current drawn from the source is greater thus requiring thicker and more expensive wires and other equipment. Therefore, power factor is a measure of the distortion from a purely resistive load. When the current and voltage are in phase, the power factor is 1.0. When the system has unity power factor (ideal case), then it means that the source has a load that obeys Ohm's Law. If both signals are sinusoidal but not in phase, the power factor is the cosine of the phase angle[HBD].

$$\text{power factor} = \frac{(\text{average power})}{(\text{rms voltage})\,(\text{rms current})} \tag{3.1}$$

With unity power factor, the total harmonic distortion (THD) is nearly zero. High power factor and low harmonics go hand-and-hand [HBD] but there is not a direct correlation. The total harmonic distortion is calculated by using eq. (3.2), where Kd is defined as the distortion factor. This distortion factor is defined in eq. (3.3). When the fundamental component of the input current is in phase with the input voltage, then $K\theta$=1. Therefore, the power factor can be defined as eq. (3.4). There are two types of PFC: passive PFC and active PFC. Passive PFC is applied by controlling the harmonic current with the use of a filter. By doing so, the nonlinear device now looks like a linear load. However, active PFC is a power electronic circuit that controls the amount of power drawn by the load in order to obtain a power factor close to unity. Active PFC controls the input current, causing it to be in phase with the voltage sinusoidal wave. Power factor correction (PFC) algorithm is implemented to help maximize the power draw from the wind turbine at a given wind speed. When dealing with non-linear loads, a rectifier stage will produce a distorted current waveform that is also out of phase with the voltage waveform. As the current becomes more out of phase with the voltage waveform, the power factor is reduced and the overall efficiency is reduced. The hardware we designed for our power inverter implements a boost-type active rectification that allows the system to run PFC. Using separate input current controllers on each phase, it is possible to produce an non-distorted current waveform that is in phase with the voltage waveform.

$$THD(\%) = 100 \times \sqrt{\frac{1}{Kd^2} - 1} \tag{3.2}$$

$$Kd = \frac{1}{\sqrt{1 + \left(\frac{THD(\%)}{100}\right)^2}} \tag{3.3}$$

$$PF = Kd \times K\theta = Kd = \frac{1}{\sqrt{1 + \left(\frac{THD(\%)}{100}\right)^2}} \tag{3.4}$$

Despite the inherit simplicity of passive PFC circuits, it suffers from some disadvantages[HBD]:

- Inductors are very bulky which restricts the usability for many applications.
- A line-voltage range is required for worldwide applications.
- By not having the voltage rail regulated, it will penalized the cost and efficiency of the DC/DC converter that follows the PFC stage

A purely resistive load is desired in order for the wind generator to operate at a maximum efficiency because a resistive load means that the system operates at unity power factor. In [III07], it states that if a generator is loaded with less than unity power factor, efficiency and capacity are lost, since more current must be sourced in order to deliver the same real power. When the voltage and current are not in phase, more current is required to deliver the same amount of power because real power is the multiplication of these two terms. Therefore, with the same amount of power delivered, the losses are much higher. The same case applies to wind turbines; if there is not a purely resistive load, higher currents will be necessary to generate the same amount of power thus producing more power losses.

In an AC/DC converter with unity power factor is the ideal power converter to charge the battery because it is necessary for the converter to approximate a resistive load. Because

it is desired to push power to the battery at all voltage levels of the turbine, the converter must be capable of boosting the voltage. The VIENNA rectifier serves as a boost, to assure that the bus voltage is always greater than the battery voltage. If the converter operates in continuous conduction mode (CCM), then it means that the current ripple is smaller than the DC current. The smaller this current ripple is, the better the efficiency.

In order to achieve unity power factor, the controller for the VIENNA rectifier should change the amount of current pulled by the converter as the input voltage changes. Therefore, the ratio between the voltage and the current should remain constant at all times. This constant ratio between the voltage and current represents the input impedance of the converter. It will allow the converter to change this ratio in order to simulate different load resistances. This way, the wind turbine will see the load as a resistor, while in reality the energy is being boosted up by the converter.

3.1 PFC vs. no PFC

In many applications, power factor correction helps reduce power transmission losses thus conserving energy, benefiting the power supply companies [OL09]. Although PFC can hurt efficiency somewhat, it can save money to these companies thus enabling them to supply more power to the end consumer. With wind turbine applications, it is also important to not only care about the electrical efficiency but the mechanical efficiency as well. Therefore, PFC is also suggested in many wind turbine converter designs. For low power applications, an AC

signal that is power factor corrected before rectification might not have a significant impact to the overall system efficiency. There are many DC/DC converters that can be designed in order to take that rectified AC power charge up a battery load at very high efficiency levels. This is why it is important to know beforehand whether PFC will significantly help us achieve high power efficiency. Before PFC analysis was started, a quick test was applied to a low power wind turbine generator that shows the significance of PFC for low power converters in wind turbine applications. A 200W turbine was driven by a DC motor in order to simulate different wind conditions. The three phase output of the turbine was first hooked to a resistive load only and the output power was measured for different wind conditions. This configuration simulates a system with unity power factor. In the same manner, the three phase generator output was connected to a three phase rectifier and the output power was also measured with same wind conditions. After comparing both power measurements, it was observed that when the turbine was directly connected to the load, an average of 15% more power was achieved. Therefore, it was concluded that for low power wind turbines application, applying power factor correction will not hurt the system's overall efficiency. It will instead increase its efficiency while considering both mechanical and electrical efficiency.

3.2 Introducing conductance (G) in the PFC algorithm

In active PFC, it makes the converter see the electronic system appear as a resistive load to the primary input source. The PFC control structure used in the VIENNA rectifier is shown

in Fig. 3.1 and it is also exhibited in [BMR98], [FC01]. This control structure is applied on each of the three phases and it consists of a multiplier that produces a current reference by multiplying the input voltage by a reference constant G, which represents the inverse resistance (or conductance) of the controller. After calculating a current reference, it is then fed to a basic compensated controller. This controller will control the individual phase of the VIENNA rectifier to keep the current in phase with the voltage at all times. The power factor correction (PFC) algorithm works by using a virtual conductance G which is defined as $1/R$. The value for this virtual conductance is commanded by the Maximum Power Point Tracking algorithm of the system as explained in chapter 4. The PFC control multiplies V_{in} by G to determine the instantaneous current reference. This current reference is then fed to a basic compensated controller which will control the VIENNA converter to keep the current in phase with the current. The PFC algorithm will also allow the converter to approximate a resistive load for the wind turbine generator. By approximating a resistive load, it minimizes the amount of energy lost to the internal resistance of the machine. Otherwise, if the current had high peaks, as in with a simply rectified AC source, the internal resistance of the machine will see higher peaks of current, which leads to higher average power loss.

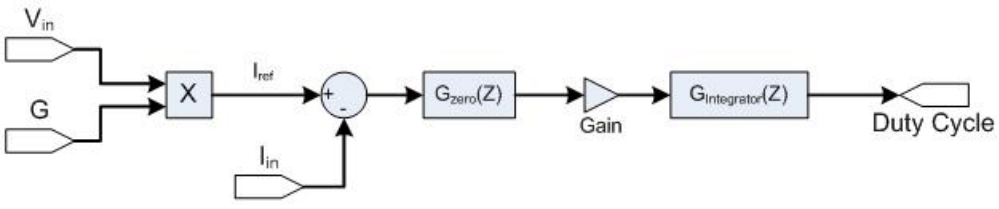

Figure 3.1: Conductance (G) PFC Algorithm

3.3 Simulating power factor correction in the VIENNA rectifier

The concept of conductance PFC algorithm was simulated using Matlab Simulink. An input current regulation model was implemented. This model includes three separate current controller for each phase. The current controller subsystem is shown in Fig. 3.2. In this figure, the current refecence is shown as ref_{var}. This variable is distributed to each of the three individual phases directly. It will assude the same refecence is set for each of the current controller loop. This reference variable is then muntiplied by each of the phases, where:

- Phase 1 = Vin_A
- Phase 2 = Vin_B. This phase is 120 degrees out of phase from Phase 1.
- Phase 3 = Vin_C. This phase is 240 degrees out of phase from Phase 2.

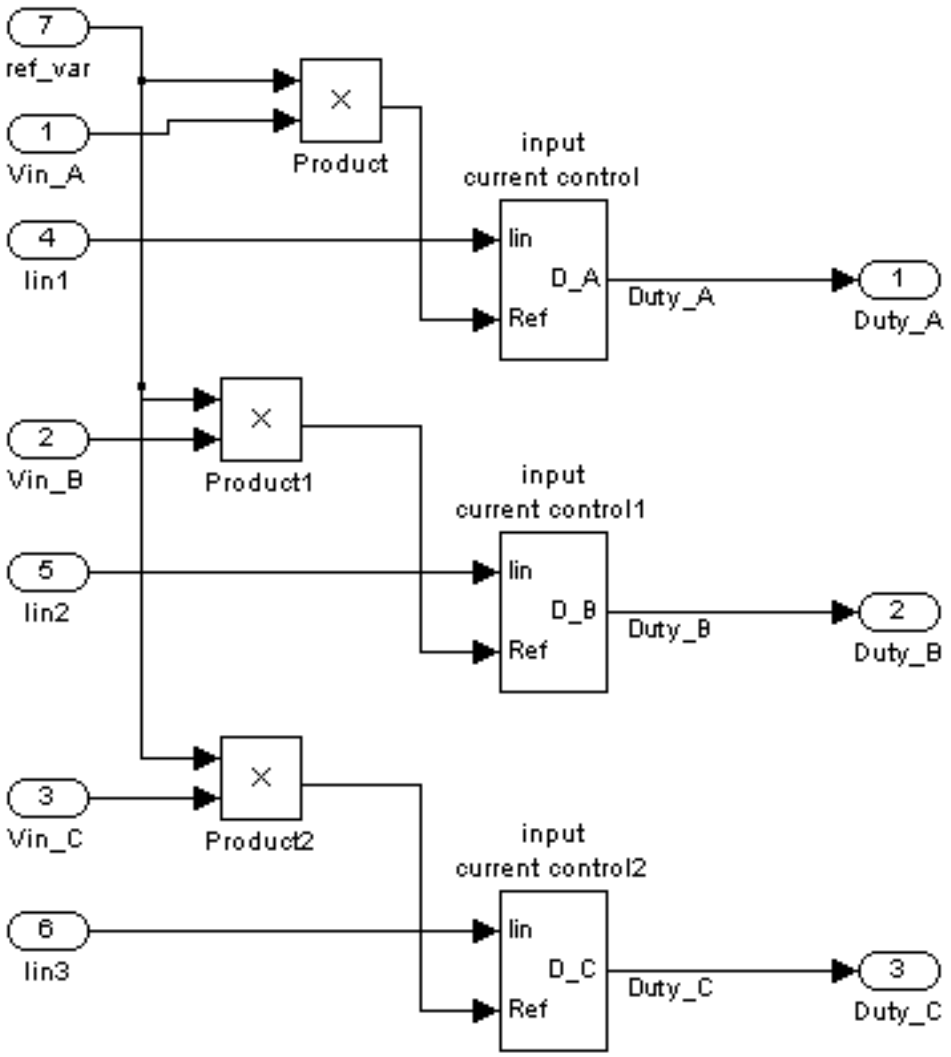

Figure 3.2: Current control model for PFC

The basic regulated controller will then take these values and calculate an optimal duty cycle for each of the phases. A model that simulates the characteristics of a wind turbine was used for the input of the converter. This turbine model is shown in Fig. 3.3. The wind speed is rampped from low to high and it is taken by the "Windmill I-V curve" subsystem. This

subsystem gives the proper rms voltage which is highly affected by the load and the current it pulls. The V_{rms} value is sent to another subsystem that creates the sinusoidal signal. The proper frequency and amplitude with the given V_rms is calculated in this subsystem. The value of the frequency depends on the type of turbine that is used. For this project, experimental results is obtained by using the "FD200W" wind turbine. Therefore, calculations for the frequency is implemented following the specific turbine equations. These equations are eq. (3.5) and eq. (3.6), where f_t is the frequency of the turbine and V_{rms} is the rms voltage of the turbine.

$$V_{rms} = 0.03773 \times RPM \tag{3.5}$$

$$RPM = 15 \times f_t \tag{3.6}$$

Solving for the frequency, we obtain eq. (3.7).

$$f_t = \frac{V_{rms}}{0.03773 \times 15} \tag{3.7}$$

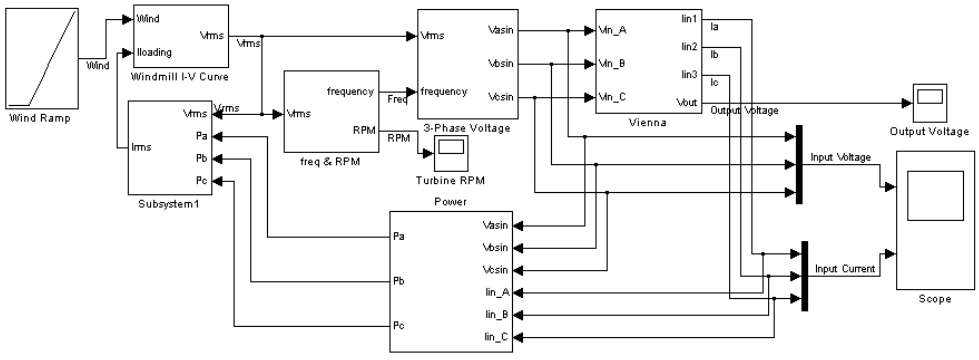

Figure 3.3: Modeling wind turbine characteristics

The input current and voltage is measured and power is calculated. This valuse, along with the rms voltage, is used to find the proper rms current. Depending on the rms current of the turbine, it will affect the rms voltage and a new frequency will be calculated. This behavior simulates accuratelly how a wind turbine reacts under different wind speed and loading conditions. This PFC control algorithm was simulated and results are shown in Fig. 3.4. This plot clearly shows the input current following the phase of the input voltage as predicted.

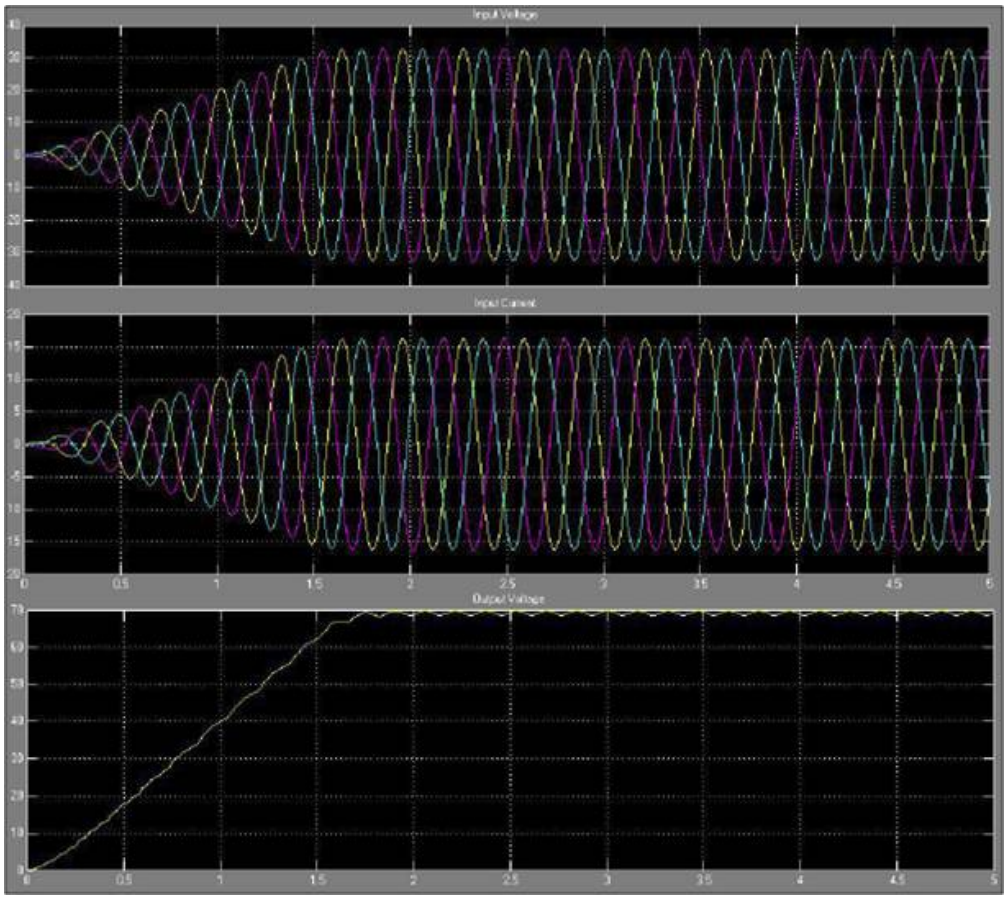

Figure 3.4: Three phase voltage (Top) and PFC current (middle) with rectified output (bottom) Matlab simulation results

This simulation shows unity power factor thus containing the same harmonic spectrum. In reality, this will never be the case because there will always be some sort of distortion in the conduction loss or small phase shift. However, these results show that the algorithm will work. Verifying the algorithm is the first step, several adjustments will be considered once it is applied onto the microcontroller.

CHAPTER 4: MPPT

Maximum Power Point Tracking (MPPT) is a widely used method, specially in PV solar power systems, in order to increase the overall energy yield. The maximum power for a wind turbine occurs at its optimum tip-speed ratio and it varies from one wind speed to another [HB08b]. Several methods have been proposed and discussed in literature [KK06][DR03][WC04]. Some of these methods require characteristic information from the turbine such as wind speed, torque, and power coefficient curve. However, they would only work well for selected turbines. The maximum power point algorithm implemented in this research does not require any external information and its being used on the rectifier stage (VIENNA). The converter will decide how much current it needs to pull depending on the type of loading. If no energy is require, MPPT will quit and the converter will keep a low rmp. By controlling the current drawn from the source, it will find an optimum tip-speed ratio and tracks the maximum power point on any given wind speed. For high power wind turbines, the maximum power is often obtained by mechanically changing the pitch angle of the blades commanded by an electrical converter that takes external readings of the current weather. Most of these turbines use blade pitch control as they calculate the optimal angle at which the blade should operate and achieve the maximum power for any wind condition. For these kind of systems, an anemometer is often required to measure the wind speed. The

reading is then sent to the electrical system of the turbine and it calculates the angle for maximum power. However, this procedure of achieving maximum power adds too many unnecessary components which increases the cost of the wind generator and electrical converter thus it is not adopted for small for small to medium power wind turbines. Several wind turbine generators also use a mechanical break system when no power is require to the electrical system. Depending of the power rating of the wind turbine, different breaking techniques are applied in order to slow down the turbine during excess wind conditions. For high power wind turbines, a mechanical rotor break is used to order to slow down the blades. With low to medium power wind turbines, when there is excess wind and the energy is no longer require, the tail forces the wind turbine to face slighly away from the wind. By causing the turbine to face away from the wind, the RPM decreases and the power of the generator decreases thus decreasing the energy of the generator. This method requires extra manufacturing costs and sometimes can be inefficient. The power for most wind turbines is characterized by its power coefficient (C_p) and the tip speed ratio (TSR). The TSR can be described as the ratio between the wind speed of the tip of the blade in respect to the actual wind speed. In simpler terms, (C_p) can be described as eq. (4.1). For a system to be 100% efficient, the blades would have to stop 100% of the wind. However, a german physicist Albert Betz proved that no wind turbine could convert more than 59.3% of the kenetic energy of the wind into mechanical energy turning a rotor [Arq09]. This proof is known as the Betz limit. Good wind turbines generally fall in the 35-45% range when converting wind

to electric energy.

$$C_p = \frac{\text{Electricity produced by the wind turbine}}{\text{Total energy available in the wind}} \tag{4.1}$$

In other words, the power coefficient characterizes the maximum aerodynamic efficiency as well as the optimal operation point of a particular turbine. Following the theory of momentum, as explained in [Mok05], for a given wind speed $v(t)$ and a rotor radius R, the power captured by a wind turbine is defined as eq. (4.2). In this equation, the air density is defined as ρ. Assuming a constant pitch angle, the power coefficient is dependent on the tip-speed ratio.

$$P_t(t) = \frac{1}{2}\rho\pi R^2 v^3(t) C_p(\lambda(t)) \tag{4.2}$$

The tip-speed ratio is defined as the ratio between the angular speed of the turbine with respect to the actual velocity as a function of time, show in eq. (4.3). Formulation of the power factor coefficient parameterized by a thrid order polynomial in $\lambda(t)$ is explained in [Mok05].

$$\lambda(t) = \frac{\omega(t) R}{v(t)} \tag{4.3}$$

Just like with solar arrays, there are two main operating regions for wind turbines as well. The right hand side (RHS) is the region at which the current draw is small while the voltage stays relatively constant. In this region, the low current draw with high input voltage will cause the turbine to spin at a higher rpm. The power in this region increases with the current and decreases with the voltage. This area is not desired because very high rpm can cause permanent damage to the blades of the generator. The left hand side (LHS) of the curve,

the current is relatively constant while the voltage decreases quickly. This time, the power is increased with voltage and decreased with current. The operation on the LHS of the curve is desired because the increase in current will cause the turbine to spin at a much slower rpm. Therefore, when the load is not present or the battery is fully charged, the converter will force the turbine to operate at the LHS. This will create a much safer operation for the wind turbine. Between these two region there is a point of maximum power. An example of a power curve is shown Figure 4.1. This curve is originated by a software developed by *ApECOR* where characterictics of a solar array is simulated. This program is extensively used in this research due to the extreme similarities the power curve of a solar array has in comparison to those of a wind turbine.

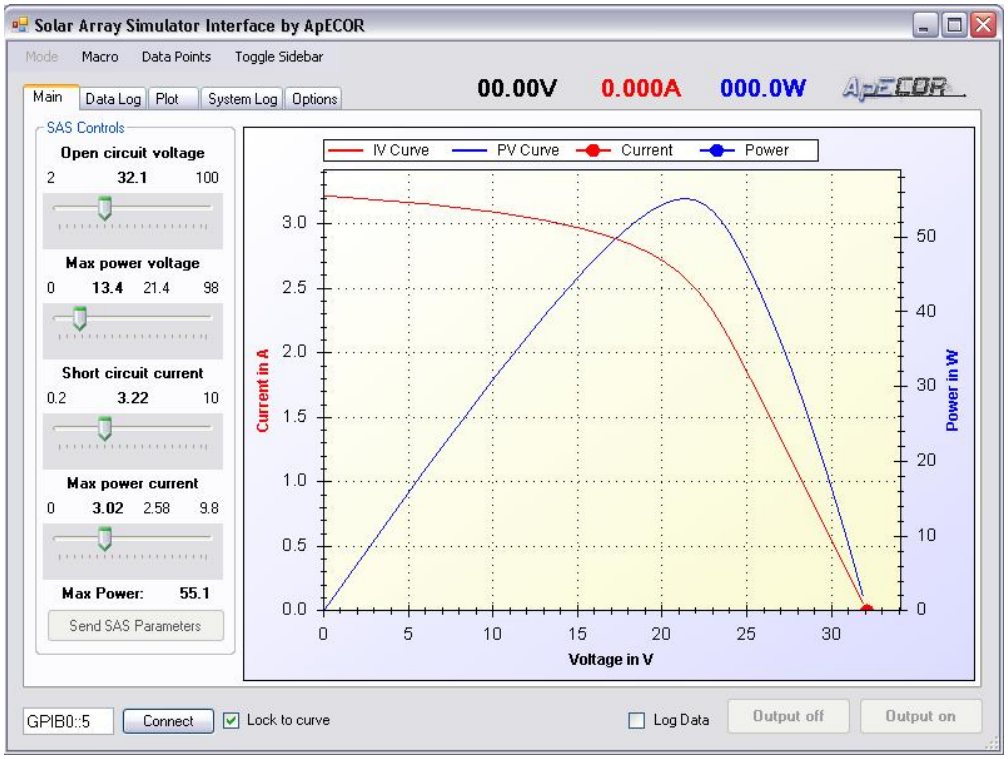

Figure 4.1: MPPT curve using the Solar Array Simulator (SAS) program developed by *ApECOR*

There are many methods for MPPT that are currently available. Some of these methods include:

1. Open/short circuit test algorithms
2. Curve scanning method
3. Hill-climbing method

For photovolatic power generation system, the use of the short current pulse is often used to measure the maximum power point [NTN00]. The current is measured thoughout this short

current period, finds the maximum value and it stays at that point until the next short current pulse. This method presents a number of drawbacks if used with wind turbines. Anothe important drawback this method presents is the power loss during the disconnection/test perio First, this method would require a knowledge of the characteristics of the wind turbine that is being used. It is unconventional to individually program every converter to fit all the existing turbines. Also, it would not be desirable to change the converter if the user decides to change the turbine type. This method also requires a periodic interruption of the current though the converter which may become difficult for turbines with higher rated power thus hurting the overall efficiency of the system. The curve scanning method is an improved version of the open/short circuit test algorithm. The load is disconnected from the turbine and it is then when the characteristic is quickly swept in order to read the entire curve of the turbine. It is then when the absolute maximum point of the curve can be easily determined. Therefore, this method does not require previous aknowledgement of the characteristic of the turbine. However, it requires longer interruption intervals and the power loss during the disconnection/test period is still present. All of these methods has been introduced for the maximum power point tracking of solar cells. If any of these methods were to be implemented on wind turbines, they would have to be modified in order to track the maximum power out of an AC source. The methods that have been proposed for wind turbines involves calculating the optimal angle speed of the generator from the measured wind speed. These methods can be effective but they require extra manufacturing cost and it is only implemented in high power wind generators. Many versions of the hill-climbing algorithm have beed used in wind

energy systems [HB08a] [HB08c] [MB04], where it explains that the powe is at its maximum when it is operation at an optimal tip-speed ratio thus varying the MPP from one wind speed to another. However, all these methods are based on the Perturb and Observe (PnO) algorithm. As defined by the power curve, the maxumim power occurs when the change in power over the change in the rotor speed is zero ($\Delta P/\Delta\omega = 0$) [HB08a]. If the algorithm detects that $\Delta P/\Delta\omega > 0$, then it will know that the maximum power point is located at a higher rpm. On the other hand, when $\Delta P/\Delta\omega < 0$, then the maximum power point is located at a lower rpm instead. This method has been widely adopted by many wind energy systems, but it presents a major drawback when a wind turbine is charging a battery. This algorithm is not set up to handle over charging protection. If a battery is charged, then the operating point will fall on the right hand side of the curve. This will make the turbine increase its rpm. For overwind conditions, this effect is undesirable because very high rmp can permanently damage the wind turbine. In high power turbines, a break system is set up for these types of condutions. For low to medium power turbines, these gear break system is not adtopted. Instead, the high rmp will cause the turbine to aim away fromt the wind. This method can also damage the turbine.

A unique way of implementing MPPT has been developed in the VIENNA converter. It consists of controlling the referece constant used in the power factor correction loop and obtain maximum power. This controller has not yet been implemented in wind turbines.

4.1 Controlling PFC constant with MPPT Algorithm

A modified version of the hill-climbing algorithm is introduced for maximum power point tracking. This algorithm uses the conductance G constant explained in section 3.2 in order to control the reference current of the ICR control. As shown in Figure 4.2, the input voltage is multiplied by a factor (G). The control loop then calculates the difference between the desired value and the real value of the commanded conductance (G) value. The MPPT algorithm will choose a G value and wait for the converter to sense the output power. This controller must be much slower in relation with the PFC controller since it has to wait for the power to settle. If this is not the case, then the power measurement can become inaccurate. Small ripple in the output power measurements may cause the converter to read a smaller power output then it actually is due to the bad timing in sampling. For example, if the first power sensed was sampled at the peak of the ripple, then a small increase in the power might still cause the lowest value of the ripple to be lower than the peak value of the previous ripple. Therefore, the lowe value will cause the controller to start going in the opposite direction since it sensed a decreased in power when in reality there was a small increase. This makes timing of the sampling to be critical. However, if the converter waits long enough for this power to settle, then timing does not become that critical. The controller will then update the appropiate duty cycle in order to maintain that error at zero.

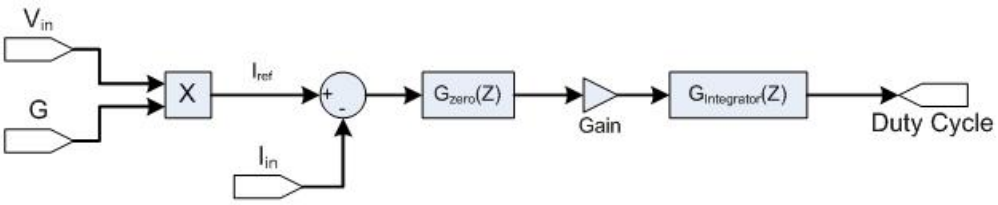

Figure 4.2: Conductance (G) algorithm for power factor correction

In a conventional hill-climbing algorithm, the duty cycle is directly updated by the MPPT controller by comparing the perturb power with the observed power. Therefore, the MPPT algorithm is designed so that it can control the input current reference constant (or conductance G). In this case of maximum power point tracking, the reference current will change and the system will re-measure the power. If there was an increase in power, then the algorithm will continue changing in the same direction. On the other hand, if there was a decrease in power, the system will change the direction at which the current reference was changed.

CHAPTER 5: DIGITAL CONTROLS

5.1 Buck-boost AC/DC converter (with bridge rectifier) controls

Different control loops were added to the buck-boost converter in order to control the input and output power of the system. The structure of these controller loops are shown in Figure 5.1. There are two main control loops: MPPT and battery charging loop. These two loops will compute a unique duty cycle. The math for the OCR loop was set to calculate a high duty cycle when the reference current is lower than the actual. It will allow the turbine to slow down when the battery is reaching the charging state. The MPPT changes the reference of the input voltage and finds the maximum power point. The most important reason behind the max function is because when the battery is charged, the voltage will start rising. Such behavior will cause an increase in the duty cycle. It is desirable to have a high duty cycle when maximum power is not needed. With high duty cycle, it forces the turbine to slow down due to the amount of current it wants to draw from the turbine.

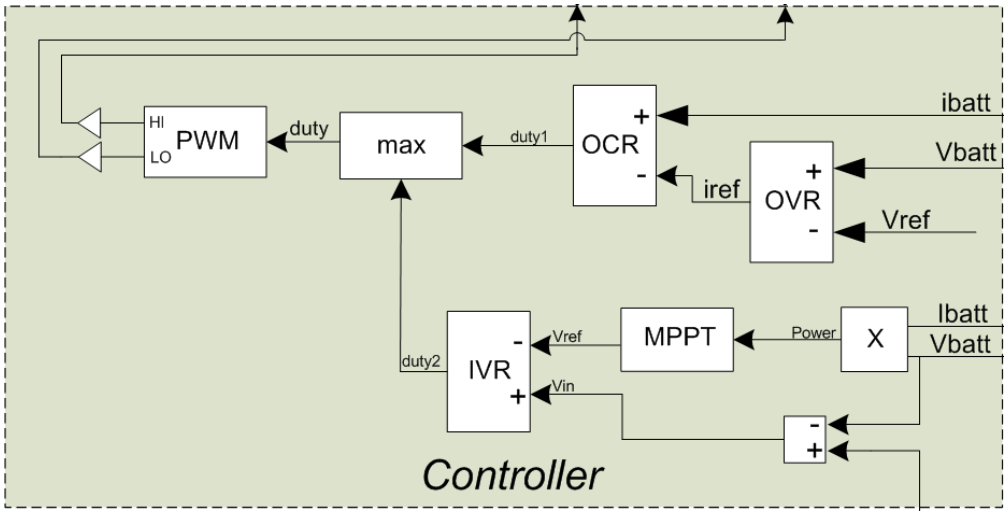

Figure 5.1: Control loops summary loop

The two inner loops are assigned to calculate two separate duty cycles. The first duty cycle, D_1, is calculated by the charging state of the battery. This loop regulates the maximum amount of power the battey when is close to the charged state. For common lithium ion batteries, the voltage raises higher than the rated voltage when the battery is charged. For example, if the rated battery voltage is 12V, the battery voltage will increase to about 15V when it is fully charged. Any higher voltage might cause permanent damage to the battery. The output voltage regulation (OVR) loop keeps track of this battery voltage. A reference value of 15V for a 12V battery is set by the microcontroller. For a 24V battery case, then the reference will be set to 26-27V.

The output of the OVR controller is zero when the battery voltage is lower than the reference voltage. The output of the OVR loop is sent to an output current regulation (OCR) loop. This OCR loop obtains the current reference value from the OVR loop. As the

battery reaches the voltage reference, the current reference is lowered. When the reference current is lower than the actual current, a high duty cycle will be commanded and less power is pushed while slowing down the turbine. The OCR will calculate the appropiate duty cycle, D_1 in order to keep a safe amout of current going to the battery.

The second duty cycle, D_2, is calculated my the maximum power point tracking algorithm (MPPT). This MPPT algorithm measures the current and voltage of the battery and find the best input voltage needed from the turbine in order to obtain maximum power. Therefore, this MPPT loop controls the input volage reference value sent to the input voltage regulator (IVR). This IVR reads the reference value assigned by the MPPT loop and it compares it with the actual input voltage measured. After this input voltage is regulated to the specified reference value, the MPPT algorithm will re-measure the power that the battery is receiving. If the power is greater than the previous measurement, then the MPPT algorithm keeps increasing the reference input voltage in the same direction. Otherwise, it will change direction and re-measure the power once more. These two duty cycle, D_1 and D_2, competes and the outter loop picks the highest one. Again, one of the main reason of picking the highest value is because at a higher duty cycle which decreases the RPM of the wind turbine. The lowering of RPM helps with the overall safety of both the converter and the turbine. For most scenarios, D_1 will be greater than D_2 when the battery does not require the maximum power the wind can provide to the system, thus lowering its speed while obtaining the same power required by the controller. In other words, D_2 is always active as long as the battery is not charged. Once the battery reaches its charged, then the system automatically drops

out of MPPT and D_1 is activated. Figure 5.2 shows a block diagram illustrating how where the controller measures the values.

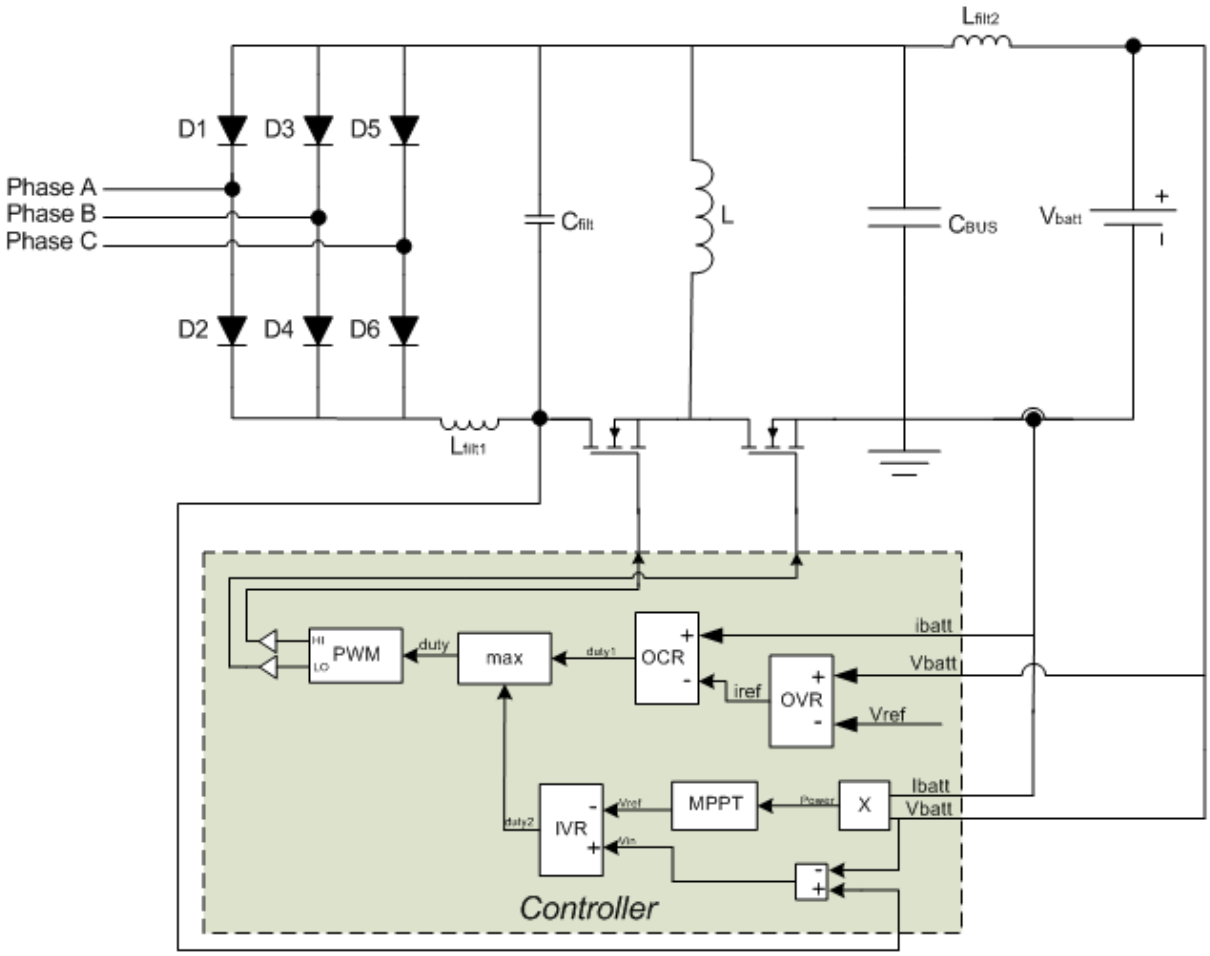

Figure 5.2: Buckboost converter with digital control loop

A summarized flow chart of the control algorithm of the buck-boost is shown in Figure A.1. Initially, the DSP checks if the wind turbine is supplying power to the converter. Depending on the amount of power supplied by the turbine and the power consummed by the load, the DSP will be able to estimate the rotor speed thus determine if it is operating at a

safe rpm. If the controller does not detect any power from the input, then it will go on stand by where every so often it will re-check the input. On the other hand, if the controller detects any power comming from the turbine, it will then initialize the system. This inicialization procedure consists of turning on the internal supply and prepare all sensing components. If no fault is detected during this procedure, the controller measures the battery voltage and it will decide whether the battery is considered full. If the battery is full, then the converter will run into OVR. Remember that OVR will be regulating the maximum battery voltage. Also, recal that this OVR loop will be controlling the output current reference which then calculates a duty cycle. If the battery is not cosidered full to the controller, then it will run the MPPT algorithimg in order to supply the maximum power available from the turbine. This loop, as mentioned earlier, will calculate a separated duty cycle. The controller will run a max function and the highest duty cycle will be passed.

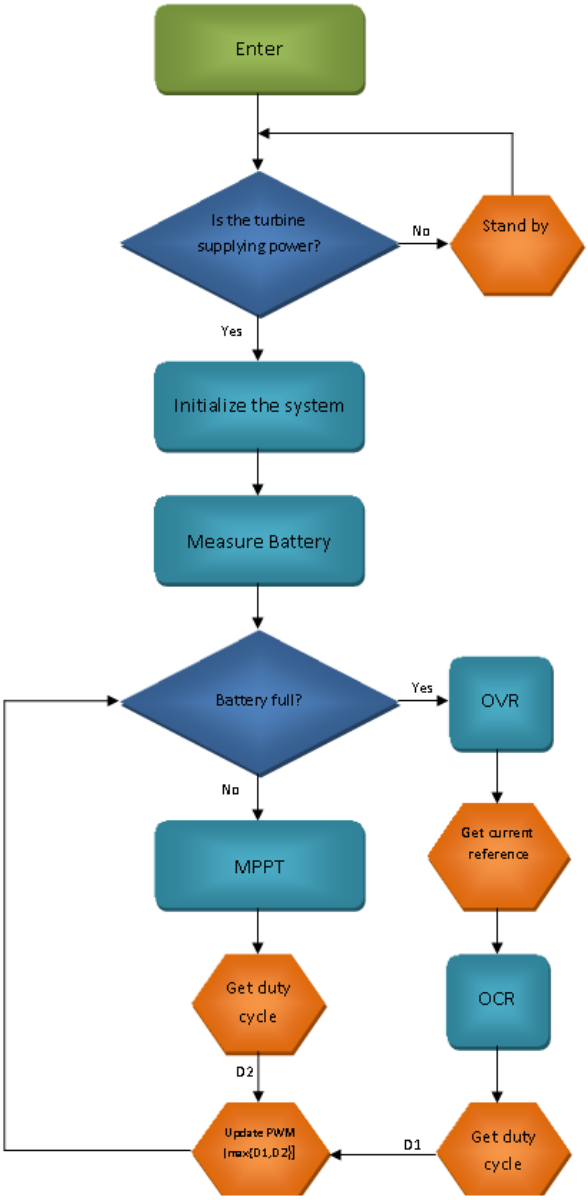

Figure 5.3: Buckboost control flowchart

The protection algorithm is simple yet very important. Initially, if the controller does not detect any battery at the output the system will remain off. This will eliminate the need of an ON/OFF button for the converter. When a 12V battery is connected to the

output, the controller then measures the output power. If this value is very low, then the controller knows that there is not enough wind to properly charge the battery. The system constantly measures the output power and decide if more power is require to the battery. If it is, then it runs the loop controls that best fit the given wind conditions in order to obtain the maximum power. On the other hand, when the battery does not need any more power, the controller will command a high duty cycle which shorts the input of the turbine thus decreasing its rmp. A flowchart of this algorithm is shown in Figure A.2.

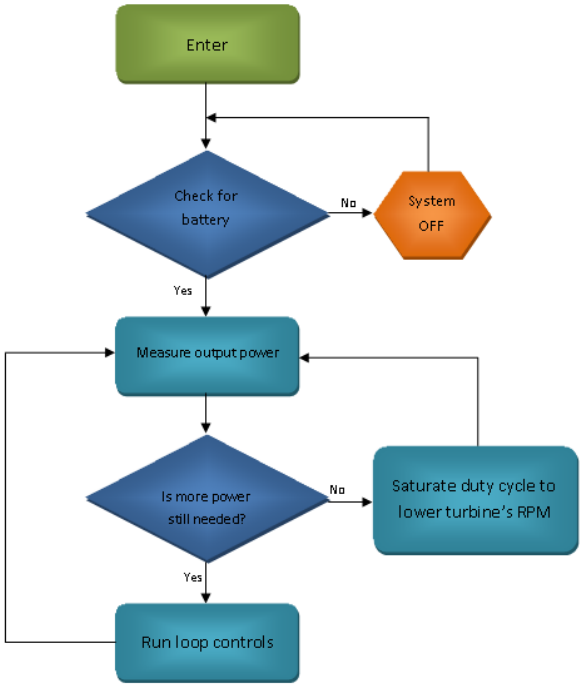

Figure 5.4: Buckboost protection algorithm flowchart

The IVR controller is a PI controller that obtains its reference from the MPPT algorithm. The reference value for this IVR is constantly changing in order to find the optimum input

voltage in order to obtain maximum power transfer. This loop commands one of the two duty cycle and the maximum value will be obtained by the main controller.

The OVR control is used for the main charging algorithm for the battery. Once the battery voltage reaches its reference, it commands a reference current value to the output current controller.

After calculating a current reference by the OVR, this loop controls the maximum amount of current the OVR allows. In other words, when the battery voltage reaches its reference value, the current reference is decreased. This commands a much lower output current. The series connection between the OVR and the OCR allows for the controller to successfully implement the battery charging algorithm. A new duty cycle is calculated and compared with the IVR duty. The maximum of these two duty cycle will be sent to the PWM controller.

5.2 VIENNA rectifier with buck converter controls

5.2.1 First stage controls: VIENNA Rectifier

Different control loops were also added to the VIENNA rectifier stage as well as the buck stage. The VIENNA rectifier is the first stage of the converter while having the buck as the second stage. There are three main controllers running on the VIENNA stage and they are as follows:

1. Power Factor Correction (PFC)

2. Maximum Power Point Tracking (MPPT)

3. Bus Voltage Regulation

The PFC algorithm has been discussed in chapter 3 and MPPT has been discussed in chapter 4.

A simplified version of how the control algorithm programmed for the VIENNA converter is shown in Figure5.5. It is composed of two main loops: one at the input and the other at the output of the VIENNA rectifier (bus). At the input of the converter, the voltage and current are sensed. This value is sent to the input current controller which, as explained in chapter 3, controls the current reference for power factor correction. The output voltage controller for the first stage controls the voltage across the bus and it is called bus voltage regulation (BVR). The BVR controller keeps this voltage at a safe value for maximum efficiency. The bus voltage will start increasing when the battery starts reaching the charged state or when the load is not present. This OVR control is necesary because an unsafe bus voltage value can cause permanent damage to the converter. The maximum duty cycle is taken mainly to make sure that we are operating on the LHS of the power curve. This will make the turbine at a slower speed when the maximum power is not needed. Remember that MPPT will command the best input current reference value that will be fed into this current controller loop.

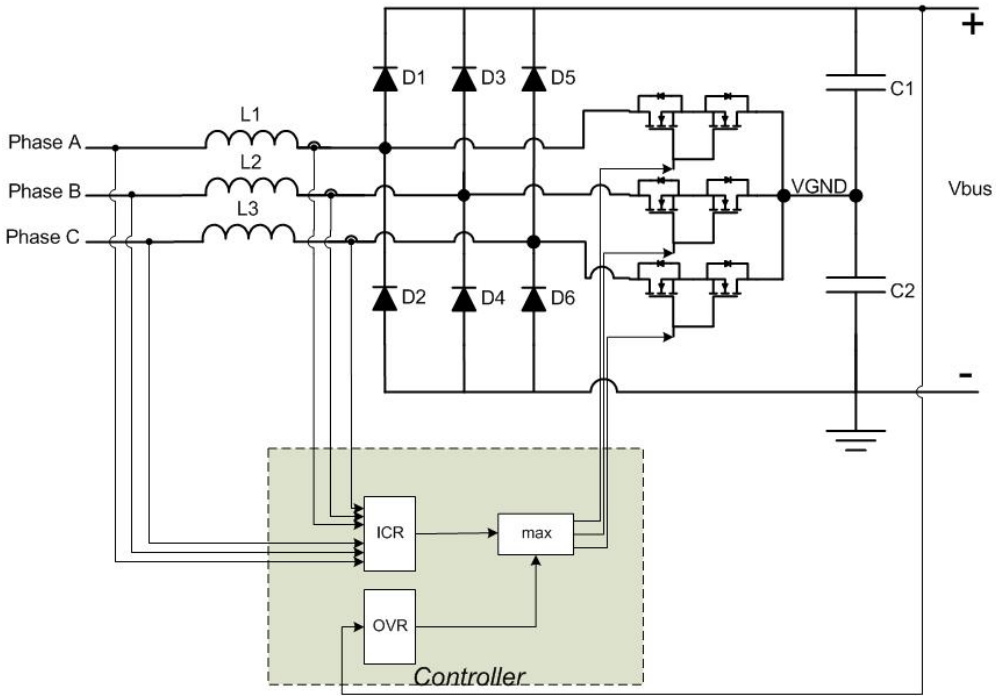

Figure 5.5: Control algorithm for the VIENNA converter (first stage)

5.2.2 Second stage controls: Buck DC/DC converter

The buck converter is the second stage of the converter and is the interface between the battery and the rectifier stage. All of the battery charge algorithms are controlled from this stage using two controller: output voltage and output current regulators. These two controlled are implemented in software using PI controllers and they work together to determine a duty cycle for the buck converter based on the status of the battery charge. The three stage charging process will be used for charging the lead acid battery and that is as follows:

1. Constant Current Mode

2. Constant Voltage Mode

3. Float Charge Mode

The current and voltage parameters for the constant current and constant voltage modes can be configured by the user based on the capacity of the battery as well as the voltage rating.

Now that there are three duty cycle producing controllers identified on the buck converter, the appropriate duty cycle must be selected according to the required response for the battery charging process. The main buck controller takes the minumum duty cycle of each of the controllers and sends it to the switching devices. The input voltage controller (bus voltage) has a voltage reference at 40 V, the output voltage controller has a 15 V reference (assuming a 12 V battery), and a current reference of 25 A for the output current controller (assuming a large capacity lead acid battery). If the converter operates at an ideal case of 100% efficiency and we are taking in 300 W of power, we would like to deliver 25 A to the battery to satisfy 300 W delivered to the battery. For smaller capacity batteries, this current reference would normally be lowered to an appropriate value according to the battery's datasheet. The overall desing of these control loops are shown in figure 5.6

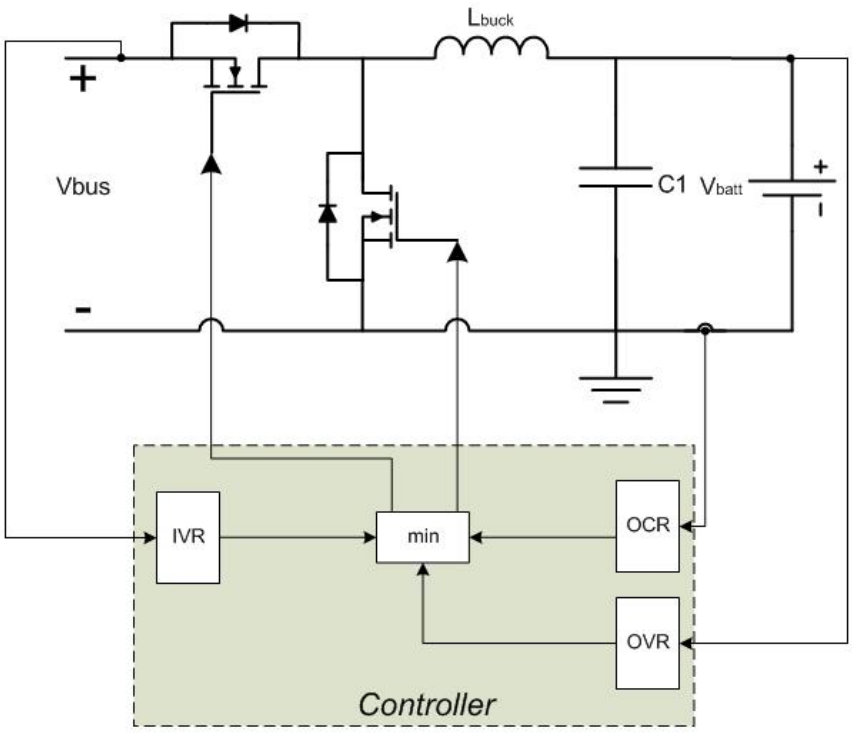

Figure 5.6: Control algorithm for the buck converter (second stage)

An advantage to using a minimum function to determine the duty cycle out of the three loops is that it inherently creates very smooth transitions in the duty cycle when moving in between the three different charging regions on the battery charge cycle. If there is no smooth transitions bewteen different duty cycles, it can cause large spikes in voltage or current causing part failure on the converter.

One of the proposed overall algorithm for the VIENNA rectifier with a buck converter is shown in Figure A.3. This algorithm is composed of two main loops as well. One of the main loop is in charge of running MPPT and calculates a current reference for the PFC algorithm. The other main loop controls runs when maximum power is not required due to the abcense

of a load or of the battery is full. Both calculated current reference will be sent to a max function of the microcontroller and power factor correction is applied with this maximum value.

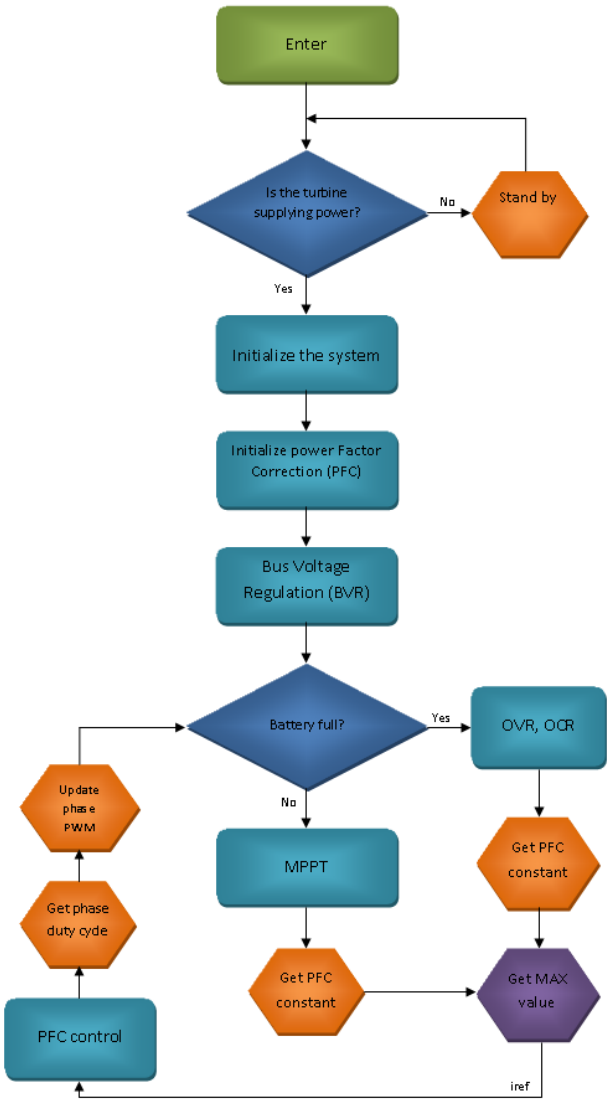

Figure 5.7: VIENNA control flowchart

Similarly, a protection loop algorithm is shown in Figure A.4, where the PFC constant is increased when no power is required from the turbine. This algorithm will control the rpm of the turbine under different current and battery conditions.

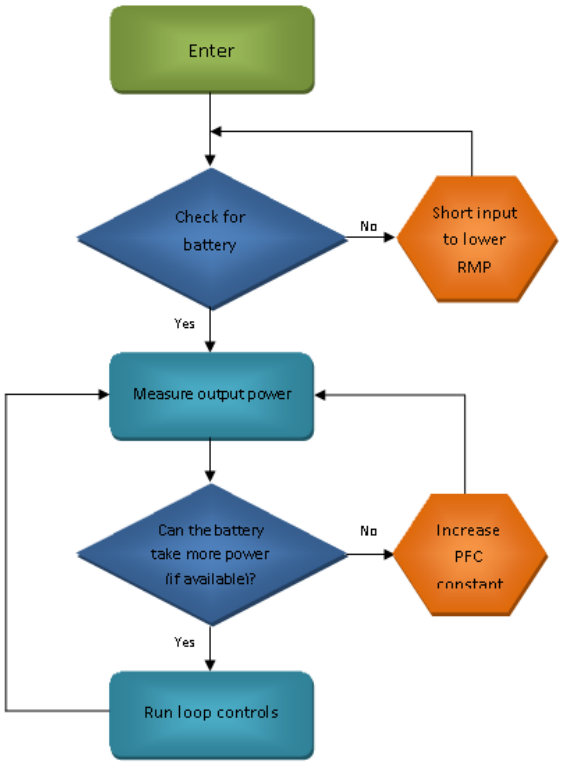

Figure 5.8: VIENNA protection algorithm flowchart

Similar to the OCR, the OVR control is a normally compensated PI controller. It is also used for the implementation of the battery charge algorithm. When the system is on the stage where the maximum current is being pushed to the battery, the voltage starts to increase. This OVR controll constantly monitors the voltage of the battery and does not let it increase to a higher voltage than the reference (15.5V for a 12 V battery as well).

Bus voltage regulation is implemented on the rectifier stage as a fail-safe method to protect the bus voltage from rising if the buck converter stops pulling power from the bus (i.e. the battery has reached a charged state). The bus voltage controller produces a current reference for the PFC control. Remember that the MPPT algorithm competes with the value calculated in this loop. The maximum of the two to be fed into the PFC algorithm. A low PFC constant results in a situation where almost no current is pulled from the turbine resulting in a fast spinning turbine and the opposite is true when the PFC constant is maximized. In order to maintain control of the wind turbine after the battery has been charged, the bus voltage will rise and the bus voltage regulation loop eventually surpasses the MPPT algorithm and the bus voltage regulation maintains a bus voltage of about 40 V.

There is a third controller that runs on the buck stage to try and regulate the bus voltage. When this converter was tested, an optimal bus voltage was found to be around 40 V. However, this value is subject to change due to efficiency control. Since the buck converter is operating as a synchronous buck converter, input voltage controller is run in order to regulate the bus voltage.

The OCR control is also a normally compensated PI controller that is mainly used for the battery charging algorithm. When the battery is on its charging state, the converter pushes as much current as it can to the battery. When the battery voltage increases to a set voltage (15.5V for a 12V battery), the OCR limits a constant current to keep the charge of the battery. This OCR control only commands a duty cycle for the second stage of the converter.

As explained earlier, the input current control is in charge of the power factor correction of the system. This controller is a normally compensated PI controller that find an optimal duty cycle in order to keep the input current in phase with the voltage. Current and voltage sensors are needed for all three of the phases. Recall that this controller calculates the reference current by multiplying this value by a factor called PFC constant. This PFC constant is obtained by a separate control loop that takes the maximum value of the output for all the other loop controls such as MPPT, OVR, BVR, and OCR. The speed of the turbine will highly depend on this constant value since higher constant will result in a much lower rpm and a lower constant value in a much higher RPM. Also, different protection algorithm will use this constant to control the power received from the turbine.

5.2.3 Different aproach for the VIENNA with buck controller

Besides the MPPT algorithm obtaining the output power information from the second stage, all the controllers for each stage are independent from each other. On the first stage, MPPT and BVR compete with each other where maximum PFC constant is used. MPPT stops working when the voltage exceedes a voltage set by BVR. When the battery is almost charged, or if there is no battery, the buck stage will stop taking the maximum power out of the bus. Therefore, the first stage independently knows when the buck is not taking as much energy by monitoring the bus voltage. Once BVR detects its reference voltage, it calculates

a higher PCF constant than MPPT. This decreases the amount of power going into the bus while slowing down the turbine.

Similarly, the second stage monitors the energy transfer to the battery in order to obey the battery charging algorithm. Therefore, IVR, OVR and OCR compete and the minimum duty cycle is used by the buck. IVR keeps a bus voltage at a lower value tan the BVR reference in the first stage. Inheretly, MPPT will run as long as IVR is the dominant loop of the second stage. Once OCR or OVR beat IVR, the bus voltage start to increase because it means that not all the power on the bus is required by the load anymore. As explained earlier, this causes BVR on the first stage to win over MPPT and the turbine will slow down and supply less power to the bus.

However, the more loops the converter has, it becomes more difficult implementing the speed of each controll loop. Another approach can be considered where both stages are dependent of each other. This new approach is shown in Figure 5.9. In this figure, the bus voltage regulation control is eliminated and MPPT now competes with the battery current controller. Both loops computes a PFC constant and a maximum fuction takes the highest of the two. This approach behaves in a similar manner than the approach previously discussed. The OCR loop will compute a low PFC constant when the battery current is below the reference. This allows the MPPT controller to find the best rotational speed at which the load will be getting the maximum current. Once the load does not require maximum current, it will increase the PFC constant to a point where the input power is enough to keep the output current at its reference.

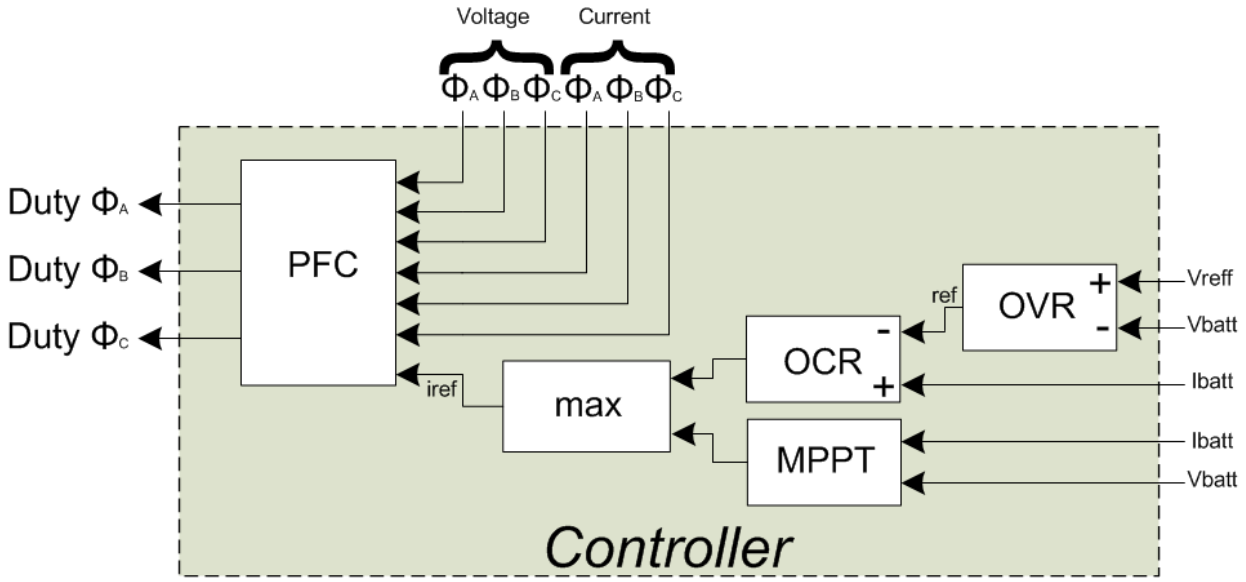

Figure 5.9: Different approach for the VIENNA with buck control loops

Because the bus voltage regulation loop is eliminated, the buck stage is the one in charge of keeping this voltage at an optimal value. This is possible because synchronous swithcing allows the buck to control its input depending on the load voltage. Because this new approach does not control the duty cycle of the buck, any of these approach could be realized:

1. Dynamic calculation of the duty cycle through input voltage regulation on the buck stage.

2. Static calculation of the duty cycle depending on the current load voltage.

The advantage of calculating a constant duty cycle is the elimination of both BVR and IVR loops which simplifies the controller significantly. However, the implementation of IVR

on the buc stage can help improve the efficiency and will adjust quickly to any unexpected changes the voltage of the load or bus.

The OVR control will regulate the output reference current for battery charging algorithm. As the battery reaches a charged state, the voltage will start to increase. The OVR will keep the voltage at about 15V. Once the battery reaches 15V, it will require a reduction in output current. This is when the battery is at the constant voltage stage. Therefore, the OVR commands a reference output current that is reduced in order to keep a 15V voltage. Also, the speed of this controller must be slower than the output current controller because it is very unlikely that the battery voltage will quickly increase in voltage by a large amount.

CHAPTER 6: EXPERIMENTAL RESULTS

6.1 Test bench and procedure

Before experimental results are shown and explained, it is important to describe how the testing procedure of the converter was done. A test bench was designed to accuratelly simulate the behavior of a wind turbine under real wind conditions. Unlike solar energy, it is almost impossible to maintain a constant wind profile while troubleshooting the converter. The use of wind tunnels is often used for these kind of tests, however, it requires extra cost and space. Therefore, the wind turbine blades were removed and the inertia of them is neglected. This allows for the wind turbine to be coupled to a DC motor with the use of a chain and different size sprockets. The sprocket size were deretmined in order to compensate for the mismatch of the maximum rpm of the DC motor and the turbine.

The DC motor operates with a maximum rotational speed of about 1700rmp and a 200W low cost wind turbine has a maximum rotational speed of about 500rpm. To lower the maximum rotational speed of the DC motor, the sprocket is the third of the size of the one attached to the wind turbine. This configuration reduces this maximum rpm value to about 567rpm max.

The power curve of a wind turbine has similar characteristics of the power curve of a solar panel. In order to estimate the location of the operating point of the wind turbine on the power curve, a solar array simulation (SAS) is used to drive the DC motor. Another important reason in using a SAS is to properly control the DC motor to control the speed of the wind turbine under different loading conditions. It is important to obtain accurate results when testing the converter, this is why it is important to simulate a similar rotational speed because it affects the input power of the converter. As mentioned earlier, when the turbine operates on the LHS, the rotational speed of the rotor will be slower than when it is operating on the RHS. The DC motor driven from a solar array simulator allows for an appropriate power curve control. The user interface of the solar array simulator, as shown in Figure6.1, allows the change in the power curve. Each power curve intales a different wind profile. Therefore, a constant wind speed can be simulated over a large amount of time.

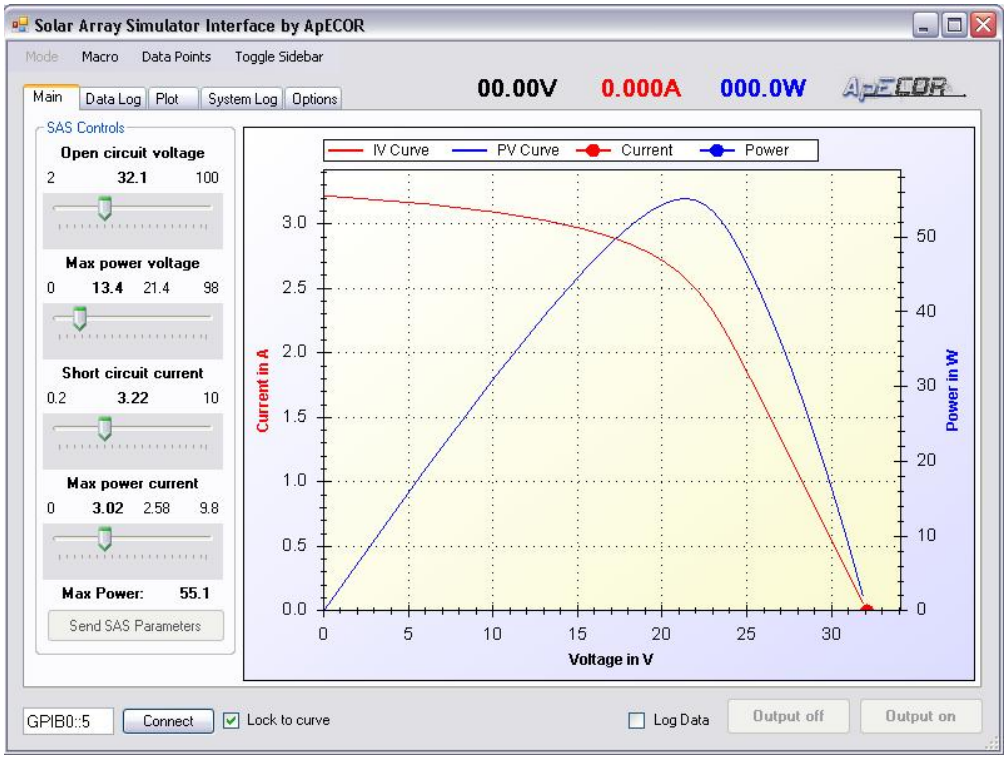

Figure 6.1: Solar Array Simulator Computer Interface

The wind turbine test bench is shown in Figure6.2. It includes a safety enclosurement that prevents any outside objects to touch the gear system since it may cause mechanical damage to the motor or turbine as well as possible injuries. In case of an emergency where an immediate shut down is require, a safety kill switch has also been installed. This kill switch cuts power from to the DC motor and quicly stops the turbine. The use of this switch does not cause any damage to the turbine or DC motor.

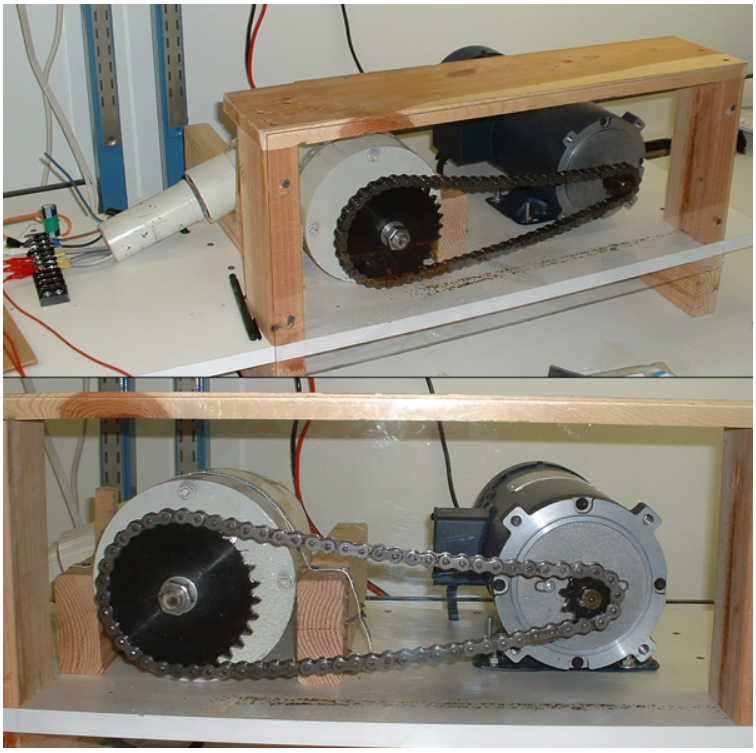

Figure 6.2: Wind Turbine Test Bench

By understanding the effects that the load and the different wind profiles has on the power curve of the turbine, this test bench is used to proper simulate a low power wind turbine without the need of a wind tunnel. The reason for the damages incurred by a constant voltage DC motor is that our PFC algorithm will continue pushing power onto our DC bus that is fed into the buck converter. Eventually, the voltage will increase to a point of total system failure and most of the components on our converter will burn out. Therefore the "Agilent E4350B Solar Array Simulator", is used to drive the DC motor that spins the wind turbine. This will give a power curve that is suitable for proper operation.

6.2 PFC experimental results

Power factor correction only applies for the the two stage three phase AC/DC converter. Figure 6.3 shows the voltage and current waveforms without the implementation a of the PFC algorithm. Because the source is not seeing the load as purely resistive, it create the current spikes which introducese more conduction loss from the turbine and it can also cause damage to the turbine.

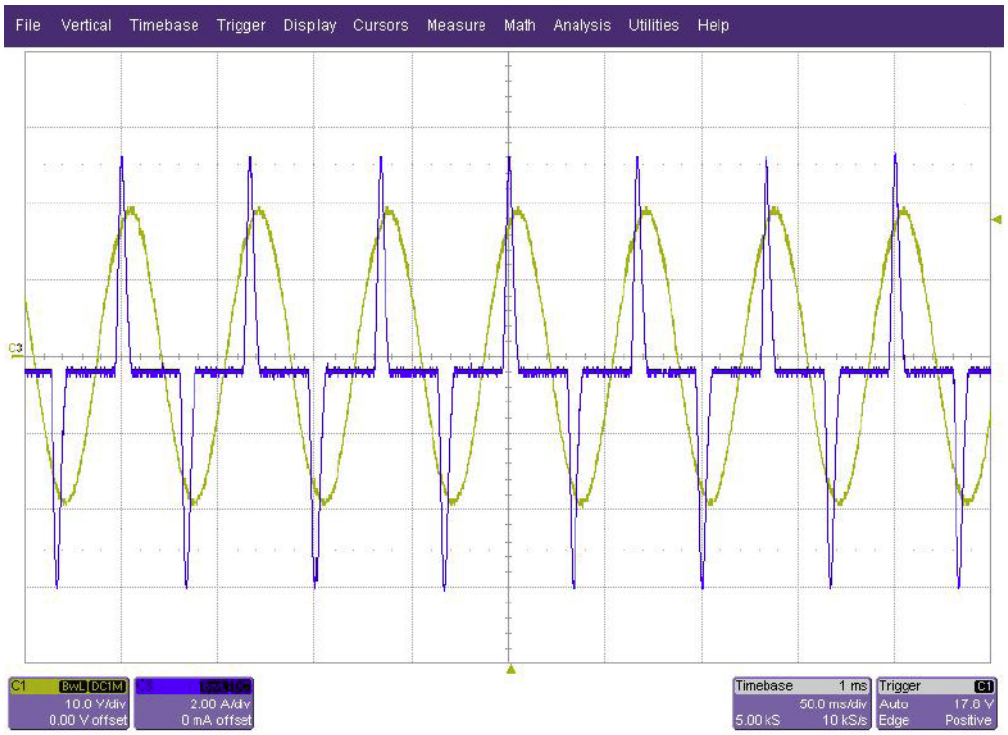

Figure 6.3: Non-Power Factor Corrected System (Voltage=Yellow,Current=Blue)

In this case, the phase capacitor maintains its voltage at approximately the peak input if the wind turbine and it waits for the next peak to recharge it. Therefore, current is drawn

from the turbine only at these peaks. Also, this pulse must contain enough energy to sustain the load until the next peak period. The converter does this by dumping a large charge into the capacitor for a very short time. The capacitor then slowly discharges the energy into the load until the next cycle repeats. It is not uncommon for the current pulse to be at 10% to 20% of the cycle duration [HBD]. This means that the current during the pulse must be at around five to ten times greater than the average current in magnitude. With the power factor correction algorithm enabled on the converter, Figure6.4 shows the input current in phase with the voltage resulting in nearly unity power factor. Therefore, it reduces conduction loss and increasing both electrical and mechanical efficiency.

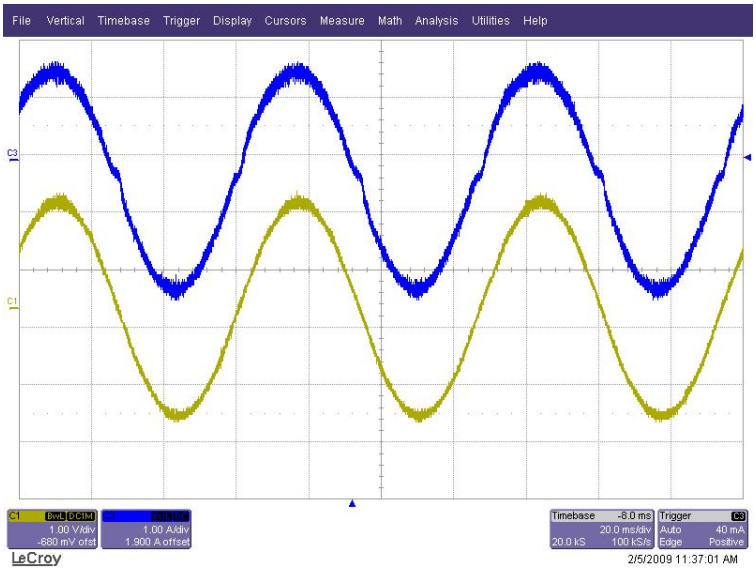

Figure 6.4: Power Factor Corrected System (Voltage=Yellow,Current=Blue)

For this case, the input current harmonics are nearly zero and can be calculated by eq. (3.4) derived in section 3. The power factor measured for the case shown in Figure 6.4

was 0.9956. Using this PF, we can solve for the THD as shown in eq. (6.2). Meaning that a power factor of 0.9956 corresponds to a THD of 9.412%

$$0.9956 = \frac{1}{\sqrt{1 + \left(\frac{THD(\%)}{100}\right)^2}} \tag{6.1}$$

$$THD(\%) = 9.412\% \tag{6.2}$$

Table 6.1 shows the power extracted from each converter. This table shows the VIENNA was able to extract extra power from the turbine. The table shows five different wind speeds. For each wind speed, both converters were compared and the maximum power extracted is observed

Table 6.1: Comparing input current under the same wind profile

	Buck-boost	**VIENNA**	**% Increase**
1	52.20 W	53.55 W	2.5
2	103.08 W	104.96 W	1.8
3	125.08 W	126.98 W	1.5
4	176.20 W	178.60 W	1.9
5	263.43 W	265.65 W	0.8

With this in mind, it is important to understand the effect of PFC under the operations of the same converter. Constant duty cycle was compared with the PFC control under the same wind profile and power level. Difference between the two were observed and it is shown in table 6.2.

Table 6.2: Comparing constant duty cycle with PFC

	Constant Duty	**PFC**
V_{batt}	15.52 V	15.68 V
I_{batt}	11.03 A	11.35 A
P_{in}	187.90 W	191.59 W
PF	0.94	0.98
P_{out}	171.18 W	177.97 W
η	91.10%	92.89%

This table shows a significant difference in the amout of power pulled from the turbine under the same wind profile. An extra 3.69 W was observed when PFC is applied. Also, the converter operated more efficient under PFC. Therefore, it can be concluded that PFC has a significant power increase with low power wind turbines.

6.3 MPPT Results

As mentioned in section 6.1, a DC motor is being used to mechanically drive the wind turbine and is ultimately simulating wind turbine conditions. The solar array simulator software was used to verify that the converter is operating at its maximum power. Remember that the power curve for a wind turbine is very similar to the power curve of a solar panel and accurate approximations can be derived from this solar array simulator. The steps of the MPPT

algorithm is be shown in Figure6.5. Each step represents a new operating PFC constant. The controller measures the battery voltage and current and finds the power delivered to the battery. A change in the PFC constant causes a change in the output power. If the new power measured is greater, then the controller keeps making changes in the same direction. On the other hand, if the new power is lower, then the controller changes the orientation of the change in the PFC constant. This is a typical behavior of a hill-climbing algorithm. These measurements in power must be slow enough to give the turbine time to react to the new conditions. Failure to do so, might result in an inaccurate measurement in the output power. One cause of this effect is the small AC ripple of the output power. It is ideal to sample the measurements in power at the peak of every ripple. Because this is not the case, quick changes in PFC constant can cause the controller to see a decrease in power while in actuallity, with enough time, the power would have been an increase. The worse case scenario would be a measurement at a absolute maximum and the next measurement was calculated at the absolute minimum of the ripple.

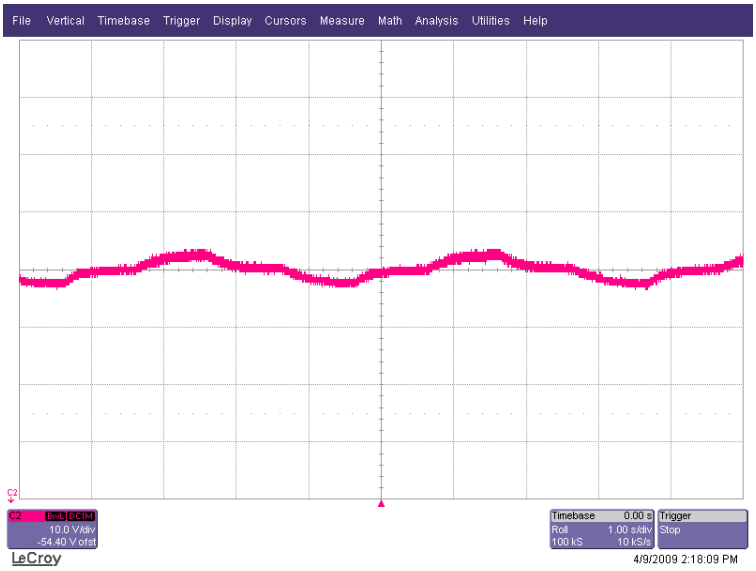

Figure 6.5: DC Motor Voltage to verify MPPT

The change in each of the step in the PFC constant must also be large enough to surpass this ripple. Because it is hard to assure sampling at the peak of each ripple, quick changes in PFC constant may also confuse the controller.

6.4 Efficiency Results

6.4.1 One stage three phase AC/DC converter

Initial testing was done in the buck-boost converter over a wide range of power level. In order to best measure the efficiency, maximum power point was simulated by manually controlling the duty cycle and place it at the MPP which varies with different wind conditions. The solar

array simulator explained earlier was used to estimate the operating point of the system. The efficiency results without any optimization can be shown in Figure 6.6. Table 6.3 shows a summary in the efficiency obtained for each power level before any optimization was done.

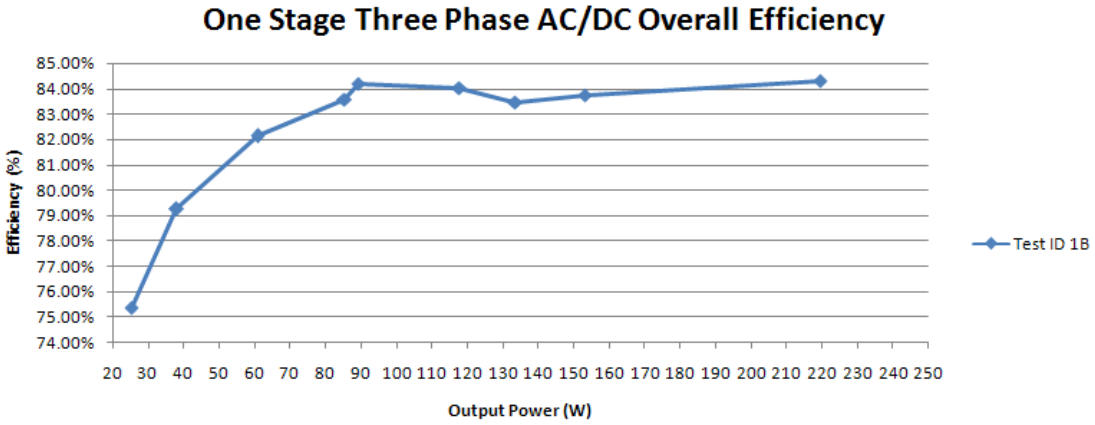

Figure 6.6: One stage three phase AC/DC converter (Buckboost) overall efficiency

Table 6.3: Buckboost converter efficiency

P_{in} **(W)**	P_{out} **(W)**	$\eta(\%)$
33.737	25.42	75.35
48.019	38.0464	79.23
74.13	60.8868	82.14
102.14	85.3644	83.58
105.81	89.1028	84.21
140.11	117.7024	84.01
159.95	133.4816	83.45
182.94	153.2084	83.75
260.19	219.3462	84.30

There are many ways to increase the overall efficiency such as finding the ideal dead time for the MOSFETS, finding the best switching frequency and the optimization of the digital controls. However, this initial efficiency results gives an idea on where the converter stands when no power factor correction is applied.

6.4.2 Two stage three phase AC/DC converter

To better analyze the two stage three phase AC/DC converter, measurements were first done at each individual stage. This will help find the largest vulnerabilities to losses in the system and allows for a much better individual diagnosis.

The testing on the VIENNA stage was done by shutting the buck converter MOSFET's off and placing a load across the bus. Three phase power was then applied to the input of the converter from a low power three phase wind turbine and the efficiency measurements were taken for a swept load, swept input power and a swept input frequency. The results in table 6.4 were compiled from testing of this first stage. The maximum efficiency for the VIENNA came out to 95.48%. In this table, an electronic load is used in order to regulate the output voltage to be at a constant value. This test was done by setting this electronic load to 40V. This is why the table shows CV as a load.

Table 6.4: VIENNA rectifier stage efficiency (CV = Constant Voltage)

f_{source} **(Hz)**	**Load**	P_{in} **(W)**	P_{out} **(W)**	η(%)
29.06	CV	103.1	96.33	93.48
29.13	CV	103.3	94.06	91.06
30.64	CV	114.0	104.09	91.28
30.69	CV	113.6	108.43	**95.48**
33.32	CV	134.4	123.09	91.58
33.43	CV	133.7	120.60	90.18
38.07	CV	171.6	163.05	95.00
37.85	CV	172.5	158.5	92.03
41.78	CV	210.2	195.16	92.84
41.91	CV	209.1	198.42	94.88
44.37	CV	242.7	223.36	92.03
44.45	CV	244.5	231.03	94.51
44.47	CV	246.8	228.77	92.68

These efficiency numbers might differ depending on how the current and voltage was measured and the accuracy of these measurement. Although accuracy is desired, these measurements are okay for individual stage testing as long as the measurements for all the testing is done the same way. This method should give a pretty good idea of the effect on efficiency when different parts are optimized. Similarly, the second stage DC/DC buck

converter efficiency was measured by applying a bus voltage higher than the battery voltage. For this case, a voltage of 40V was applied to the bus since it has proven to be a reasonable range for obtaining good efficiency for this particular converter. Table 6.5 shows the results of the second stage of the converter (Buck stage).

Table 6.5: Buck DC/DC converter stage efficiency

V_{in}(**V**)	I_{in}(**A**)	P_{out}(**W**)	η(%)
39.97	1.85	68.169	92.19
40.01	1.67	61.799	92.28
40.17	1.69	61.851	91.12
40.25	2.47	94.091	94.65
40.26	2.46	94.941	**95.86**
40.24	2.57	95.911	92.75
40.10	2.56	96.531	94.03
39.94	2.38	88.651	93.26
40.23	2.31	87.301	93.94
40.08	2.93	108.26	92.19
40.06	3.33	124.23	93.13
40.03	3.59	133.05	92.59
40.02	3.92	145.51	92.76
39.98	4.42	163.32	92.42
40.13	4.41	164.54	92.98

Although the efficiency for each individual stage is high, the overall efficiency is not so great since it is determined by eq. (6.3). For the whole system to have an efficiency greater than 90%, both stages must be operating at about 95% or higher. Because this is not the case, each stage must be optimized in order to reach an overall efficiency of 90% or higher.

$$\eta_{overall} = \eta_{vienna} \times \eta_{buck} \tag{6.3}$$

Different tests were implemented, each with a unique change in parts in order to observe any efficiency change. One major change was the use of the DSP. These individual efficiencies were taken using two DSP, one for each phase. We were able to take way one of the DSPs and implement all the controls in one DSP. Each test were defined by an test ID number. The description of some of test ID is shown in Table 6.4.2

Table 6.6: Test ID description

Test ID	VIENNA MOSFETs	Buck MOSFETs	Other Hardware Changes	Comments
10	IRFZ48Z	IRF4410	One DSP only	Bus voltage regulation of 40V
11	IRFZ48Z	IRF4410	One DSP only	Bus voltage regulation of 35V
12	IRFZ48Z	IRF4410	One DSP only	Bus voltage regulation of 30V
13	IRL2910	IRF4410	No gate diode	Bus voltage regulation of 35V; Buck driver components modified
14	IRL2910	IRF4410	With gate diode	Bus voltage regulation of 35V; Buck driver components modified
15	IRFZ48Z	IRF4410	VIENNA MOSFETS	Bus voltage regulation of 35V; Buck driver components modified

16	IRFZ48Z	IRF4410	-	Bus voltage regulation of 40V; No MPPT; Buck driver components modified
17	IRFZ48Z	IRF4410	Increased input inductance	Bus voltage regulation of 40V; No MPPT
18	IRFZ48Z	IRF4410	Changed input inductor cores	Bus voltage regulation of 40V; No MPPT
19	IRFZ48Z	IRF4410	-	$F_{sw} = 50kHz$
20	IRFZ48Z	IRF4410	Changed buck inductor core	$F_{sw} = 50kHz$

Before any modifications, the maximum overall efficiency was about 87.8% at a power level close to 200W. Now, with these new modifications, the efficiency is reaching 90% at a 110W power level. The improvements of efficiency between some of these test cases is illustrated in Figure 6.7. The measurements on the efficiency for all of the cases were done the same way to avoid any diviation in the results. This plot shows the potential of this two stage converter when it is optimized. Note that test ID 13 through test ID 16 comments some modifications in the buck driver components. These modifications were the diode on the output of the high side gate driver pin. During one of the testing, the buck driver (LM5101A) stopped driving the high side. Initially, it appeared to be due to the current that feeded back to the gate PIN. Therefore, the diode was removed and the driver was

replaced. Test results showed a slight decrease in efficiency when this diode is populated. However, the change in efficiency is not very significant.

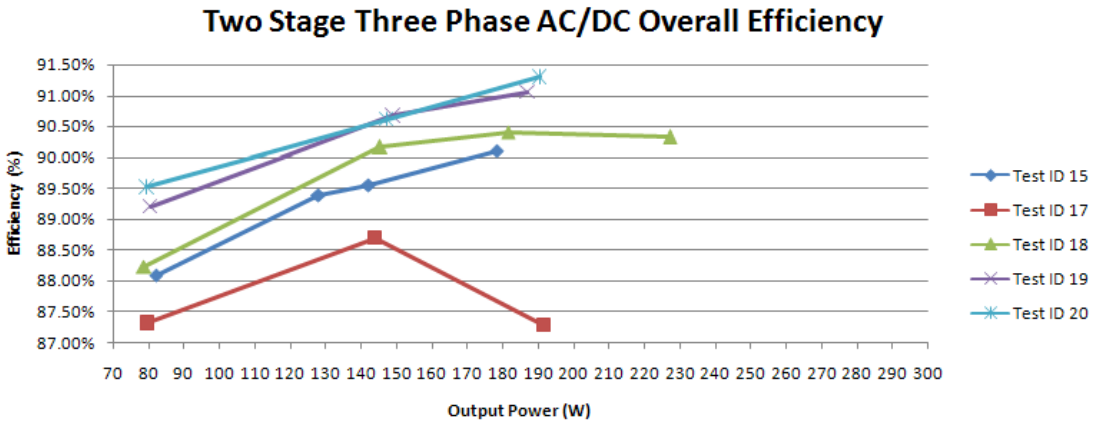

Figure 6.7: Two stage three phase AC/DC converter (VIENNA rectifier with Buck) overall efficiency

6.5 Converter Hardware

The first prototype of the buck-boost converter is shown in Figure 6.8. This is only the first prototype for this design and it has a lot of room for improvement. It operates using one DSP (not shown in the figure) and the component count is minimal. The second prototype will include a much compact design with some layout and component improvements. However, it gives an overall perspective on where it stands when compared to the VIENNA converter.

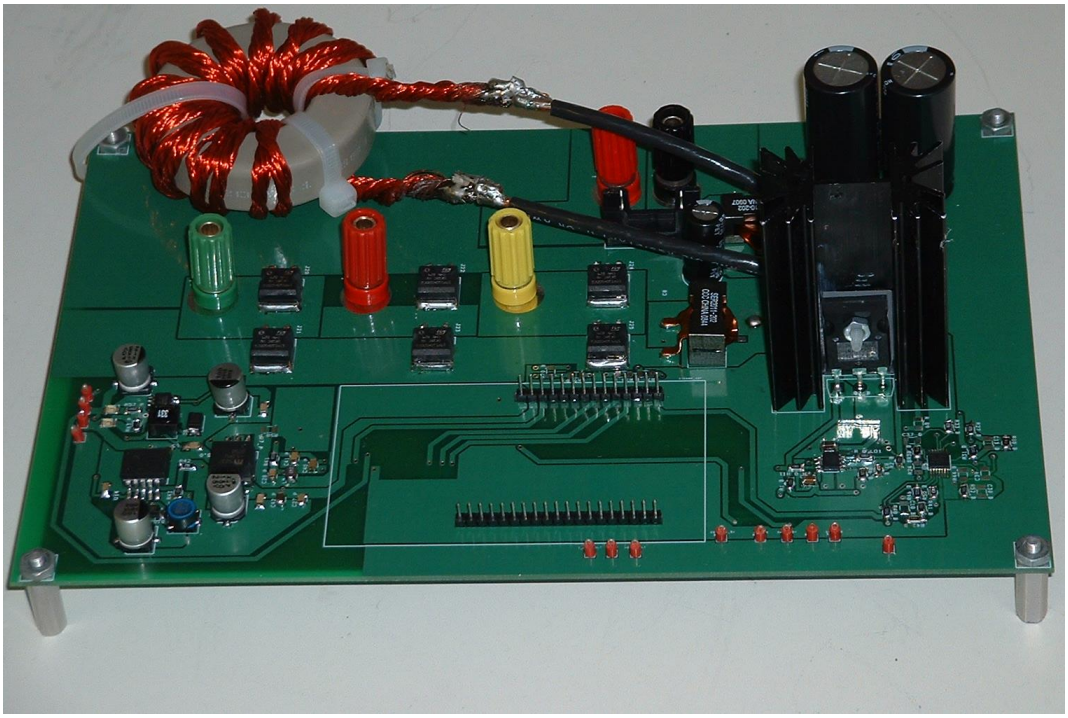

Figure 6.8: Buck-boost converter (first prototype)

On the other hand, the VIENNA converter is on its thrid prototype. The top view of this converter, shown in Figure 6.9, includes four inductors (one for the second stage and three for the first stage). This side also includes all the switching devices as well as the capacitors for the bus and the three phases. The bottom view, shown in Figure 6.10, includes all the sensing and power supply components. It has a slighly large component count which increases cost. However, the price ramains under $25 per unit count for high quantities. Initially, this converter was designed to power all the components from the battery. If the battery does not have enought charge to power all the components, the converter will fail to

operate. This thrid prototype powers the bus from the input thus not requiring any battery voltage for initial start up.

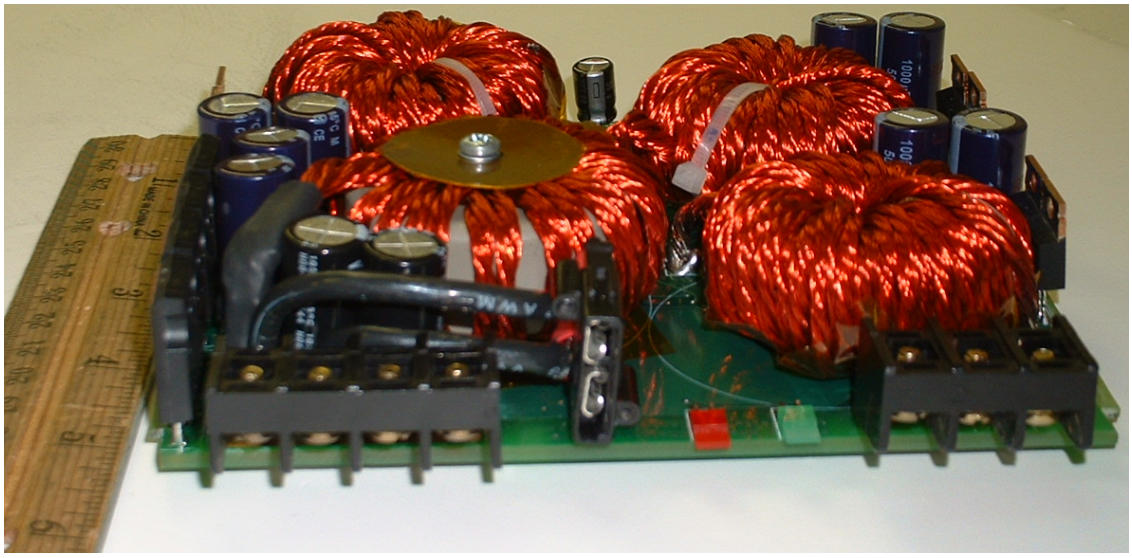

Figure 6.9: VIENNA with buck converter (third prototype: Top view)

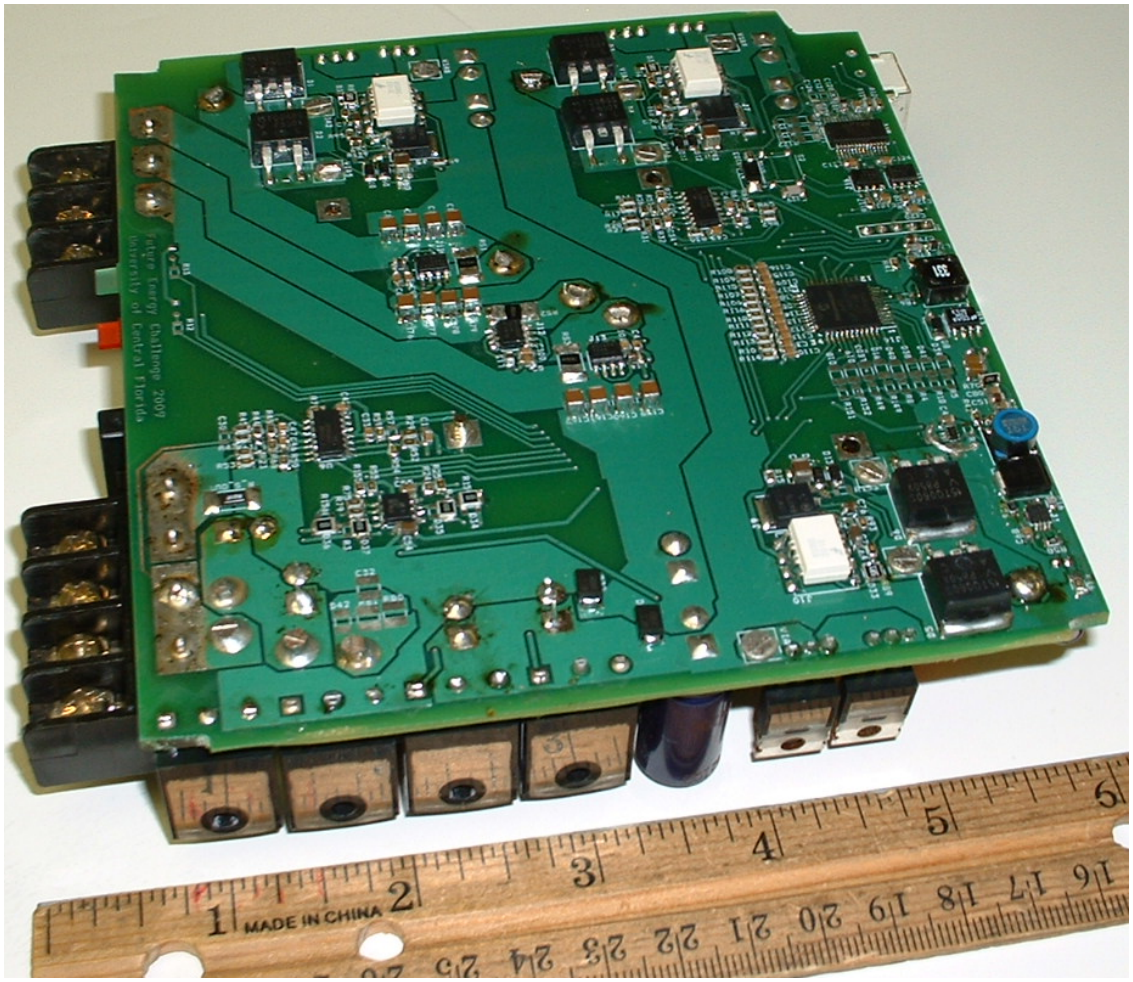

Figure 6.10: VIENNA with buck converter (third prototype: Bottom view)

CHAPTER 7: CONCLUSION

Wind energy research has become an area of high interest for power electronics. The use of low cost and low power wind turbines for personal use has a very low demand due to the poor efficiency of the power transfer to the load. The advantage of having a load appear as purely resistive as opposed to a switched load is that a purely resistive load can significantly increase the maximum power transfer. The implementation of power factor correction has only been proposed for high power wind turbines, which limits the use for a regular household. However, it is important to understand the effect PFC has when it is applied in low and medium power wind turbines.

Different control loops than can be realized in wind power converters have been discussed in detail, all of them offering a safe battery charging algorithm where the RPM of the turbine is controlled by the converter. Over-wind and over-power protection was implemented without the use of a dump load. Two different control loop approaches for the two stage three phase AC/DC converter was discussed. One of the approaches offers independence between the two stages. The second approach proposes dependence between between the stages, where bus voltage regulation is eliminated. Two options were considered for controlling the duty cycle of the second stage: static and dynamic.

Both types of converters discussed had the same implementation for the MPPT algorithm. This algorithm includes a basic hill-climbing method where the change in PFC constant causes a change in output power. Depending on the direction of this change, the controller continues changing the PFC constant if there was an increase in power, or it will change the direction of change in PFC constant if there was a decrease in power. Also, both converters were designed to be at the lowest cost possible, each under $25 for high quantities.

Therefore, by considering the use of power factor correction and maximum power point tracking, high efficiency can be obtained from low to medium power wind turbines at a low cost. Because there are certain areas that do not have significant wind activity, a low costing, small wind turbine would be beneficial. Building a large, expensive turbine would not provide adequate benefit to the cost involved. However, a small, inexpensive wind turbine would provide additional power to the area at a lower cost than alternative energy sources.

APPENDIX A: FLOWCHARTS

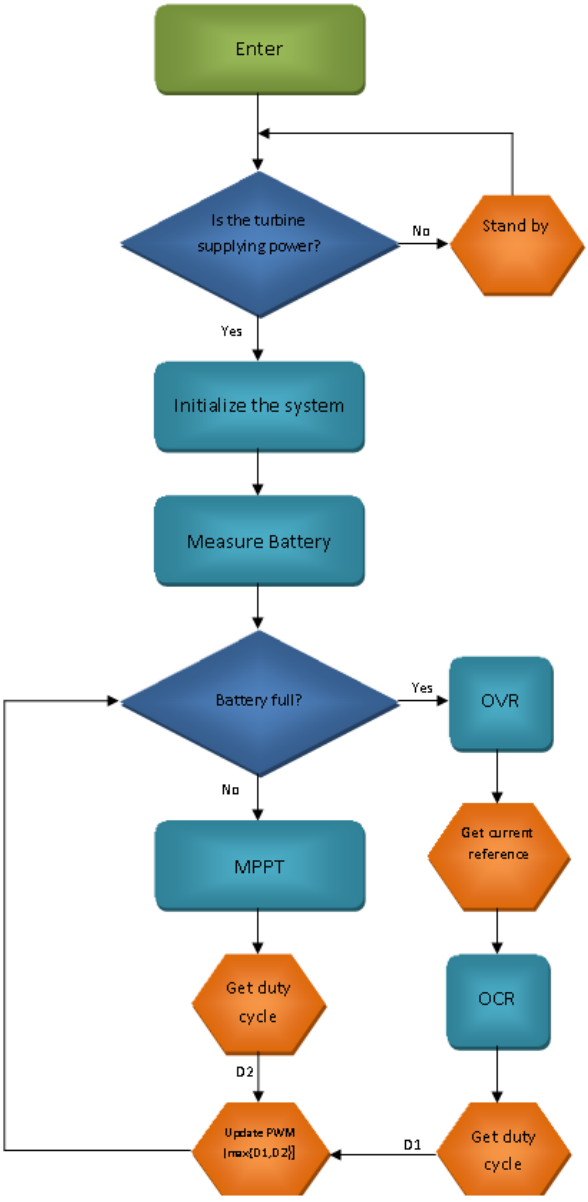

Figure A.1: Buckboost control flowchart

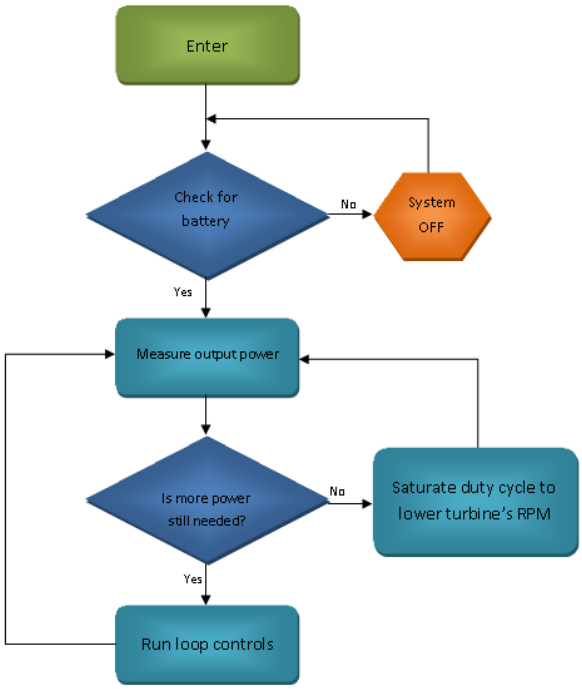

Figure A.2: Buckboost protection algorithm flowchart

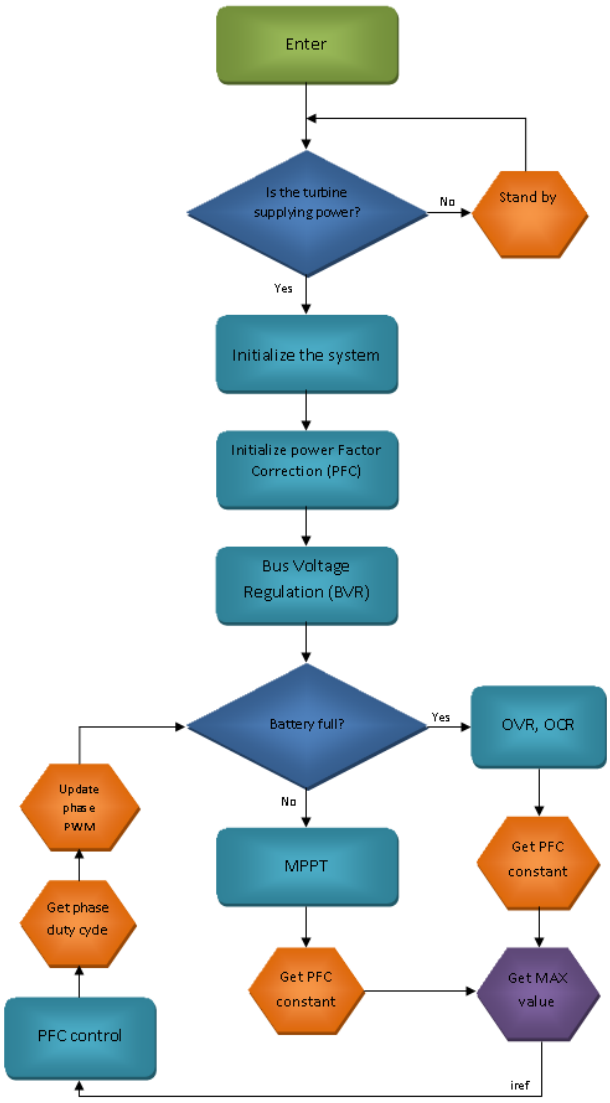

Figure A.3: VIENNA control flowchart

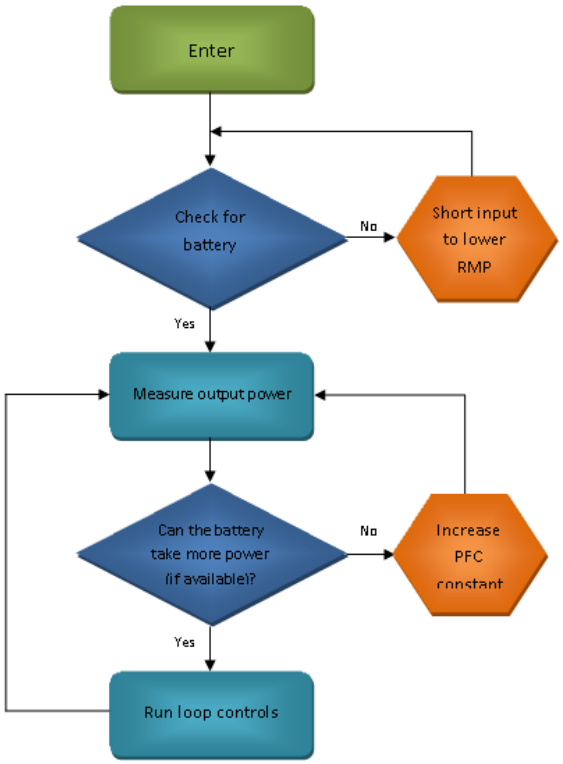

Figure A.4: VIENNA protection algorithm flowchart

APPENDIX B: EQUATIONS

Topology Research

Buck-boost converter (MODE 1):

$$\frac{d}{dt}I_L = \frac{V_{in}(t)}{L} \tag{B.1}$$

$$i_L = \frac{V_{in}DT}{L} + I_L(0) \tag{B.2}$$

Buck-boost converter (MODE 2):

$$\frac{d}{dt}I_L = \frac{V_o(t)}{L} \tag{B.3}$$

$$i_L = \int_0^{(1-D)T} \frac{V_o}{L}dt = \frac{V_o\,(1-D)\,T}{L} \tag{B.4}$$

$$\Delta I_{L_{mode1}} + I_{L_{mode2}} = 0 \tag{B.5}$$

$$\frac{V_{in}DT}{L} + \frac{V_o(t)}{L} = 0 \tag{B.6}$$

$$\frac{V_o}{V_{in}} = -\left(\frac{D}{1-D}\right) \tag{B.7}$$

$$i_{in} = D * i_L \tag{B.8}$$

$$i_L = \frac{V_{in}D - V_o\,(1-D)}{sL} \tag{B.9}$$

$$i_c = i_{diode} - I_o \tag{B.10}$$

$$i_{diode} = (1-D)\,i_L \tag{B.11}$$

$$I_o = (1-D)\,i_L - I_o \tag{B.12}$$

VIENNA rectifier with a buck converter:

$$i_L = \frac{V_{in}(t)}{L} + I_L(0) \tag{B.13}$$

$$i_L = \frac{1}{L}\,(V_{in} - V_o)\,(t - DT) + I_L(DT) \tag{B.14}$$

$$\frac{V_o}{V_{in}} = \frac{1}{1-D} \tag{B.15}$$

On-Resistance of a power MOSFET:

$$R_{DS(on)} = R_{source} + R_{ch} + R_A + R_J + R_D + R_{sub} + R_{wcml} \tag{B.16}$$

Switching power loss for a power MOSFET:

$$P_{SW} = \frac{1}{2} I_D V_D \left(t_{off} + t_{on}\right) f + \frac{1}{2} C_{oss} V_D^2 f \tag{B.17}$$

Output capacitance of a power MOSFET:

$$C_{OSS} = C_{GD} + C_{DS} \tag{B.18}$$

Turn on/off time of a power MOSFET:

$$t_{on} = t_{off} = \frac{Q_{sw}}{I_G} \tag{B.19}$$

Ohms Law:

$$I = \frac{V}{R} \tag{B.20}$$

Sensing calculations:

$$V_{DC_{offset}} = \frac{R_{38}}{R_{38} + R_{24}} V_{5V_{filtered}} \tag{B.21}$$

$$A_v = \frac{R_b}{R_a} \tag{B.22}$$

$$\frac{5V}{60V} = \frac{R_{18}}{120k\Omega} \tag{B.23}$$

$$R_{18} = 120k\Omega \times \frac{5V}{60V} = 10k\Omega \tag{B.24}$$

Power Factor Correction (PFC):

$$\text{power factor} = \frac{(\text{average power})}{(\text{rms voltage})\,(\text{rms current})} \tag{B.25}$$

Total Harmonic Distortion (THD):

$$THD(\%) = 100 \times \sqrt{\frac{1}{Kd^2} - 1} \tag{B.26}$$

$$Kd = \frac{1}{\sqrt{1 + \left(\frac{THD(\%)}{100}\right)^2}} \tag{B.27}$$

$$PF = Kd \times K\theta = Kd = \frac{1}{\sqrt{1 + \left(\frac{THD(\%)}{100}\right)^2}} \tag{B.28}$$

Wind turbine equations for the FD200W model:

$$V_{rms} = 0.03773 \times RPM \tag{B.29}$$

$$RPM = 15 \times f_t \tag{B.30}$$

$$f_t = \frac{V_{rms}}{0.03773 \times 15} \tag{B.31}$$

Power Coefficient (C_p) equation for a wind turbine:

$$C_p = \frac{\text{Electricity produced by the wind turbine}}{\text{Total energy available in the wind}} \tag{B.32}$$

Power equation for a wind turbine:

$$P_t\,(t) = \frac{1}{2}\rho\pi R^2 v^3(t) C_p\,(\lambda\,(t)) \tag{B.33}$$

Tip-speed ratio equation:

$$\lambda\,(t) = \frac{\omega\,(t)\,R}{v\,(t)} \tag{B.34}$$

LIST OF REFERENCES

[Arq09] Michael Arquin. "Wind Energy Math Calculations: Understanding Coefficient of Power (Cp) and Betz Limit.", 2009. [Online; accessed 1-June-2009].

[Bal08] B. Jayant Baliga. *Fundamentals of Power Semiconductor Devices*. Springer Science, New York, first edition, 2008.

[Bar] Vrej Barkhordarian. *Power MOSFET Basics*. International Rectifier.

[Bat04] Issa Batarseh. *Power Electronic Circuits*. John Wiley and Sons, Inc, New Jersey, first edition, 2004.

[BLP07] R. Burgos, R. Lai, Y. Pei, F. Wang, D. Boroyevich, and J. Pou. "Space Vector Modulation for Vienna-Type Rectifiers Based on the Equivalence between Two- and Three-Level Converters: A Carrier-Based Implementation." In *Power Electronics Specialists Conference, 2007. PESC 2007. IEEE*, pp. 2861–2867, June 2007.

[BMR98] S. Buso, P. Mattavelli, L. Rossetto, and G. Spiazzi. "Simple digital control improving dynamic performance of power factor preregulators." *Power Electronics, IEEE Transactions on*, **13**(5):814–823, Sep 1998.

[Che05] Wai-Kai Chen. *The Electrical Engineering Handbook*. Academic Press, illustrated edition, 2005.

[DR03] R. Datta and V.T. Ranganathan. "A method of tracking the peak power points for a variable speed wind energy conversion system." *Energy Conversion, IEEE Transactions on*, **18**(1):163–168, Mar 2003.

[FC01] M. Fu and Q. Chen. "A DSP based controller for power factor correction (PFC) in a rectifier circuit." volume 1, pp. 144–149 vol.1, 2001.

[HB08a] J. Hui and A. Bakhshai. "Adaptive algorithm for fast maximum power point tracking in wind energy systems." pp. 2119–2124, Nov. 2008.

[HB08b] J. Hui and A. Bakhshai. "A new adaptive control algorithm for maximum power point tracking for wind energy conversion systems." In *Power Electronics Specialists Conference, 2008. PESC 2008. IEEE*, pp. 4003–4007, June 2008.

[HB08c] J. Hui and A. Bakhshai. "A new adaptive control algorithm for maximum power point tracking for wind energy conversion systems." pp. 4003–4007, June 2008.

[HBD] HBD853/D. *Power Factor Correction (PFC) Handbook*. ON Semiconductor.

[III07] John C. Elmes III. *"Maximum Energy Harvesting Control For Oscillating Energy Harvesting Systems."*. Master's thesis, University of Central Florida, 2007.

[JXC06] Z. John Shen, Yali Xiong, Xu Cheng, Yue Fu, and P. Kumar. "Power MOSFET Switching Loss Analysis: A New Insight." volume 3, pp. 1438–1442, Oct. 2006.

[KA02] H.Y. Kanaan and K. Al-Haddad. "A new multiple-loops control scheme for a three-phase/switch/level PWM rectifier based on the input/output feedback linearization technique." volume 2, pp. 1404–1409 vol.2, Nov. 2002.

[KEZ96] J.W. Kolar, H. Ertl, and F.C. Zach. "Design and experimental investigation of a three-phase high power density high efficiency unity power factor PWM (VIENNA) rectifier employing a novel integrated power semiconductor module." In *Applied Power Electronics Conference and Exposition, 1996. APEC '96. Conference Proceedings 1996., Eleventh Annual*, volume 2, pp. 514–523 vol.2, Mar 1996.

[KK06] E. Koutroulis and K. Kalaitzakis. "Design of a maximum power tracking system for wind-energy-conversion applications." *Industrial Electronics, IEEE Transactions on*, **53**(2):486–494, April 2006.

[KZ97] J.W. Kolar and F.C. Zach. "A novel three-phase utility interface minimizing line current harmonics of high-power telecommunications rectifier modules." *Industrial Electronics, IEEE Transactions on*, **44**(4):456–467, Aug 1997.

[MB04] G.D. Moor and H.J. Beukes. "Maximum power point trackers for wind turbines." volume 3, pp. 2044–2049 Vol.3, June 2004.

[Mok05] K. Mok. "Identification of the power coefficient of wind turbines." pp. 2078–2082 Vol. 2, June 2005.

[NTN00] T. Noguchi, S. Togashi, and R. Nakamoto. "Short-current pulse based adaptive maximum-power-point tracking for photovoltaic power generation system." volume 1, pp. 157–162 vol.1, 2000.

[OL09] Michael OLoughlin. "Why is PFC Important?", 2009. [Online; accessed 27-May-2009].

[WC04] Quincy Wang and Liuchen Chang. "An intelligent maximum power extraction algorithm for inverter-based variable speed wind turbine systems." *Power Electronics, IEEE Transactions on*, **19**(5):1242–1249, Sept. 2004.

[YA07] N.B.H. Youssef and K. Al-Haddad. "Experimental Implementation of a New Quasi-Linear Control Technique on a 1.5 kW Three-Phase Boost-Type Vienna Rectifier." pp. 497–502, June 2007.

[YAK06] N.B.H. Youssef, K. Al-Haddad, and H.Y. Kanaan. "DSP Based Experimental Validation Technique Applied to the Development of a New Vienna Rectifier Small Signal Model." pp. 394–399, Nov. 2006.